X-810-72-282
PREPRINT

NASA TM X- 66060

AMPLITUDE FADING OF SIMULTANEOUS TRANSIONOSPHERIC L-BAND AND VHF SIGNALS RECEIVED AT THE GEOMAGNETIC EQUATOR

JUNE 1972

GSFC — GODDARD SPACE FLIGHT CENTER
GREENBELT, MARYLAND

X-810-72-282

AMPLITUDE FADING OF SIMULTANEOUS TRANSIONOSPHERIC L-BAND AND VHF SIGNALS RECEIVED AT THE GEOMAGNETIC EQUATOR

W. B. Sessions*

June 1972

* Westinghouse Electric Corporation

GODDARD SPACE FLIGHT CENTER
Greenbelt, Maryland

AMPLITUDE FADING OF SIMULTANEOUS TRANSIONSOPHERIC L-BAND AND VHF SIGNALS RECEIVED AT THE GEOMAGNETIC EQUATOR

W. B. Sessions

ABSTRACT

At Ancon, Peru, simultaneous observations of 1550-MHz and 136-MHz signals from the ATS-5 and INTELSAT-I spacecraft show ionospheric fading as great as 27 dB at 136 MHz, and 6 dB at 1550 MHz. The observations were made on 48 days during the 1970 autumnal and 1971 vernal equinox periods. Comparison of the two frequencies, in respect to rates and depths of fades, is made.

Statistical distributions of the received signal levels during ionospheric scintillation occurrences are presented which may be of use to communications system engineers with operational requirements in the equatorial regions. The distributions show that during expected periods of scintillation, the L-band signal typically falls 1.1 dB below the median for 1.0 percent of the time, and the VHF signal falls 11.5 dB below the median for 1.0 percent of the time.

CONTENTS

ILLUSTRATIONS

ILLUSTRATIONS (continued)

ILLUSTRATIONS (continued)

ILLUSTRATIONS (continued)

AMPLITUDE FADING OF SIMULTANEOUS TRANSIONOSPHERIC L-BAND AND VHF SIGNALS RECEIVED AT THE GEOMAGNETIC EQUATOR

INTRODUCTION

In the fall of 1970, a series of measurements began at the satellite tracking station at Ancon, Peru, whereby personnel from the Instituto Geofisico del Peru, under the cognizance of NASA/GSFC, recorded simultaneous VHF (136 MHz) and L-band (1550 MHz) signals received from INTELSAT-I and ATS-5 synchronous satellites. The measurements were taken with the intent of providing an additional data base from which to further study the effects of the ionosphere on radio-wave propagation, particularly at L-band frequencies.

This report presents the results of observations taken on 48 days during the 1970 fall and 1971 spring equinox period. Significant scintillation occurred at both VHF and L-band on 60 percent of the measurements.

The general signature characteristics of ionospheric scintillation is discussed. Cumulative amplitude distributions that provide statistics on the received power levels relative to the median level are presented. These statistics could be useful to system designers with equatorial region operational requirements.

DATA ACQUISITION

The station at Ancon, Peru (coordinates 11°46'S, 76°52'W), monitored the L-band and VHF signals simultaneously through two separate receivers. The receiver AGC (automatic gain control) voltages, indicative of signal strength, were recorded on magnetic tape and sent to NASA/GSFC for further processing. The L-band signal was received from ATS 5 at 1550 MHz through a receiver with a 10-kHz bandwidth and an AGC time constant of 30 milliseconds. The VHF signal was received from two separate sources. From September 29, 1970, through October 22, 1970, the VHF signal was received from INTELSAT-I at a frequency of 136.44 MHz. After September 29, 1970, the VHF signal was received from the ATS-5 spacecraft at a frequency of 136.47 MHz. The test configuration for the L-band and VHF systems are shown in Appendix A (Figures A-1 and A-2).

A typical test run, or pass, lasted approximately 2 hours. Each pass began by calibrating the system and recording the calibration signal on the magnetic tape for use in data processing. Immediately following the calibration, the data signals were recorded for approximately 1 hour. The systems were again calibrated, data were recorded for another hour, and then a final calibration was made.

The times of observation were specifically selected to maximize the probability of taking data when scintillation could be observed. Reports by Golden[1] and Aarons, et al.,[2] indicate that equatorial ionospheric scintillation is seasonal in nature, with periods about the equinoxes showing high-scintillation activity. In addition, scintillation appears to be nocturnal. Accordingly, the measurements began September 29, 1970, just after the fall equinox, and continued through November 6, 1970. A second series of measurements began March 11, 1971, just before the vernal equinox, and continued through April 9, 1971. Both series of observations were made during local nighttime hours. Figures 1 and 2 show the observation intervals, and provide information on a day-by-day basis as to when amplitude fluctuations occurred.

Figure 3 shows the two recorded signals. The VHF signal is a continuous carrier. However, difficulties encountered during insertion of the ATS-5 spacecraft into orbit resulted in ATS 5 spinning about an axis approximately parallel with the earth's axis, with a spin period of about 787 milliseconds. As a result, the L-band signal is received in energy pulsations for 52 milliseconds (3-dB points) as the spacecraft antenna pattern sweeps across the ground-receiving system.

DATA PROCESSING

The analog tapes recorded in Peru are shipped to GSFC for processing. The tapes are played back, demodulated, and fed into a 14-bit analog-to-digital converter where the signals are digitized and sampled at a rate of 200 samples per second. The digital values are then recorded on a seven-track digital magnetic tape for further processing. The demodulated analog signals which are fed to the analog-to-digital converter are simultaneously recorded on paper charts. These analog recordings are available for analysis, and they provide an identifying source for which digital tapes should be processed on the computer. Tapes with greater than 1-dB level variations were thus selected to be processed on the IBM 360-91.

The tapes recorded for days on which scintillation occurred were processed by automated techniques, using an IBM 360-91 computer in conjunction with software developed by Westinghouse Electric Corporation.[3] The calibrations in each data channel are automatically detected and the information is used to assign the proper magnitude to each data sample. Data are then processed to determine the frequency distribution and cumulative distribution of the signal levels for both L-band and VHF.

Each VHF data point (every 5 milliseconds) is used in processing the VHF statistics. Due to the pulsing nature of the L-band signal shown in Figure 3,

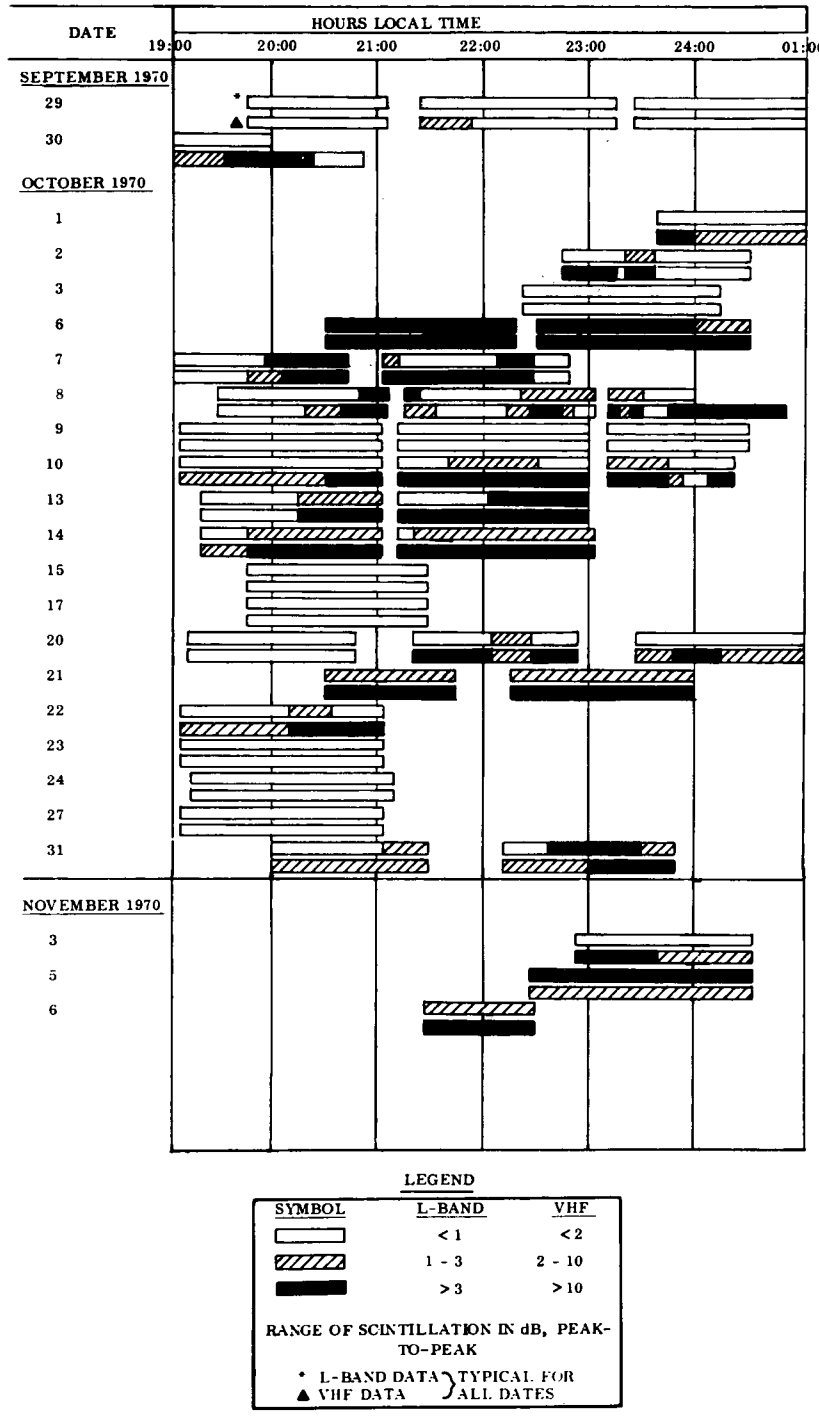

Figure 1. Hours and Peak-To-Peak Range of Ionospheric Scintillation Observed at Ancon, Peru, During the 1970 Fall Equinox

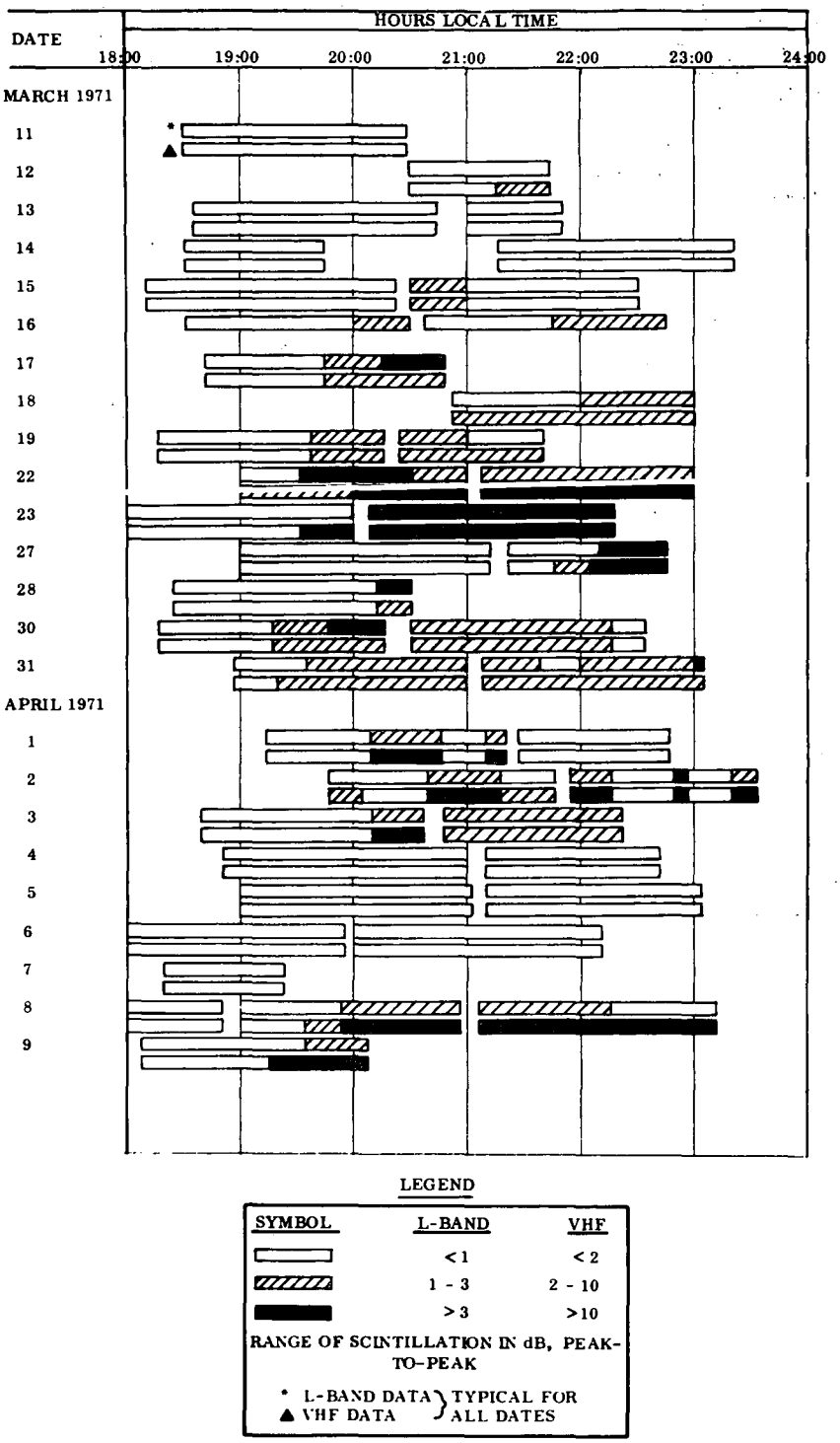

Figure 2. Hours and Peak-To-Peak Range of Ionospheric Scintillation Observed at Ancon, Peru, During the 1971 Spring Equinox

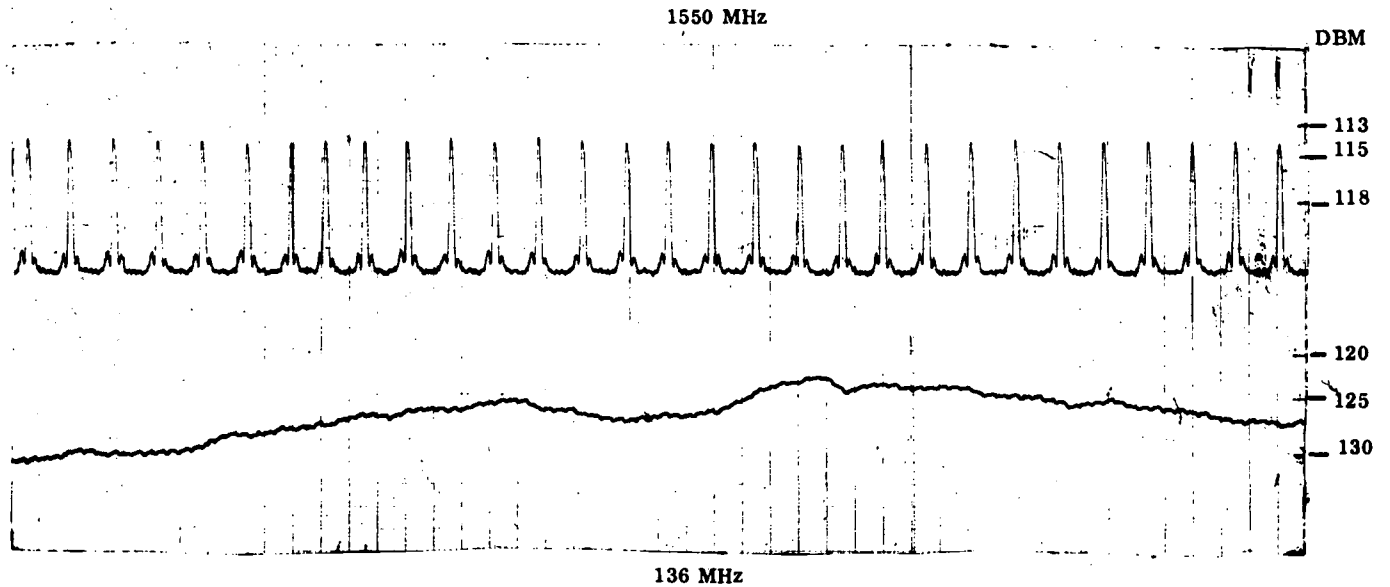

Figure 3. Ionospheric Disturbance of VHF and L-Band Signals

the amplitudes at the center of the L-band pulses were used in processing the L-band statistics. The computer program selects the proper L-band sample for processing by using the known geometrical characteristics of the pulse.

EXPERIMENTAL RESULTS

Figures 1 and 2 show a summary of the observation times covered by this report. Results of data taken over 48 days are presented. As shown, on 34 days, significant VHF scintillation occurred; and on 28 days, L-band scintillation of magnitude greater than 1 dB occurred. Peak-to-peak magnitudes of L-band scintillation as large as 6 dB and VHF scintillation as large as 27 dB were observed. During the autumn equinox, the initiation of L-band scintillation had a tendency to be delayed from the onset of VHF scintillation (Figure 1). October 7, 8, 10, and 14 are examples of days that exhibited this delay. During the autumn equinox, the ATS-5 spacecraft was the signal source for L-band, and INTELSAT-I was the signal source for VHF. In scintillation occurrence, this time delay for the two signals may be caused by the different subionospheric intersection points of ATS 5 and INTELSAT I. However, the difference is only slight because the elevation angles of the two satellites from Ancon are on the order of 55 degrees and within 5 degrees of each other.

Figure 4 shows occurrence of scintillation on March 22, 1971. The record shows that the onset of scintillation is generally abrupt, a fact noted by other observers.[2] Cessation of scintillation and other changes in state (changes in amplitude levels and changes in rates of scintillation) were also noted to occur in a sudden manner. In many instances, it was also noted that, on the order of an hour after the initial burst of scintillation, a relatively quiet period would exist after which the magnitude would increase again. Figure 4 also shows that the beginning and ending of L-band scintillation occurred simultaneously with the starting and stopping of VHF scintillation. In this particular record, L-band and VHF signals were from the same source, ATS 5.

The recording in Figure 5 also shows an interesting observation, i.e., a change in state of the VHF scintillation at approximately 19:44 hours local time at the receiving station. Before 19:44 hours, the VHF scintillation occurred at a relatively slow rate of variation with peak-to-peak amplitudes of 15 dB. At 19:44 hours, the rate of scintillation increased, and the peak-to-peak amplitude decreased to approximately 8 dB. Also at 19:44 hours, the magnitude of the L-band scintillation increased to approximately 3 dB. Although the VHF amplitude variations decreased, the L-band amplitude variations increased. Evaluation of all the analog recordings indicated that the most active L-band scintillation periods occurred when the VHF rate of scintillation was generally similar to that shown after 19:44 hours on Figure 5. The magnitude of L-band scintillation thus appears to be correlated with the rate of VHF scintillations.

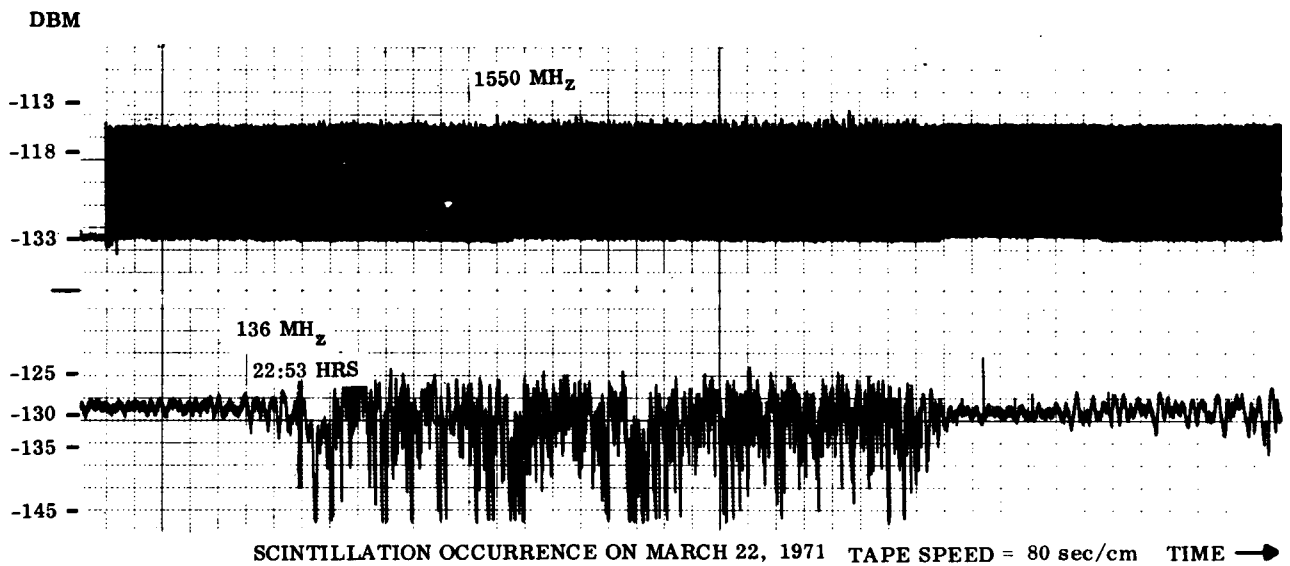

Figure 4. Record of Simultaneous L-Band and VHF Signals Received From ATS 5 on March 22, 1971

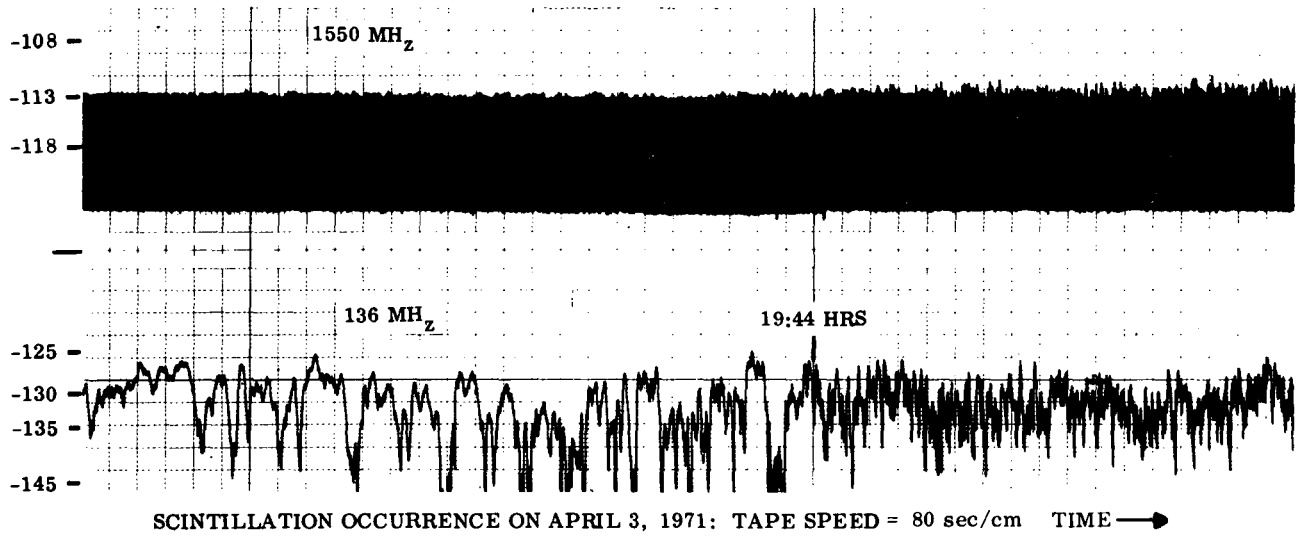

Figure 5. Record of Simultaneous L-Band and VHF Signals Received From ATS 5 on April 3, 1971

Appendix B shows the cumulative amplitude distributions of 28 individual passes for which scintillation occurred. These distributions were computed using the GSFC IBM-360/91 computer. The cumulative distributions shown in Figure 6 are typical of those observed during the 1970 autumnal equinox. Figure 7 shows typical cumulative distributions for the 1971 vernal equinox period. As shown, the distributions for the two equinox periods are similar. For more than 2 hours during the expected periods of scintillation, the L-band signal level typically falls 1.1 dB below the median for 1.0 percent of the time and 1.8 dB below the median for 0.1 percent of the time.

CONCLUSIONS

The behavior of L-band and VHF ionospheric scintillation in the equatorial region during the expected worst months of a year has been observed. L-band peak-to-peak variations as large as 6 dB, and VHF peak-to-peak excursions as large as 27 dB, can occur. The statistical distributions indicate that ionospheric scintillation at L-band frequencies is large enough to influence the design of systems operating in equatorial regions having requirements for high reliability.

Some relationships between L-band and VHF scintillation were observed that may be significant in providing more insight to the physical phenomenon which causes ionospheric scintillation. Simultaneous measurement of the two signals resulted in the following observations:

- L-band fading was always accompanied by VHF fading.
- L-band fading occurred when VHF fading was present for 73 percent of the time.
- The change-of-state (e. g., onset, etc.) of L-band fading was similar to the established VHF fading characteristics.
- L-band-fading amplitude was greater when the VHF fading rate was high, indicating correlation between L-band amplitude and VHF rate of fade.
- L-band and VHF scintillation occurred simultaneously when the signals emanated from the same source, indicating that the same physical mechanism may be responsible at both frequencies.

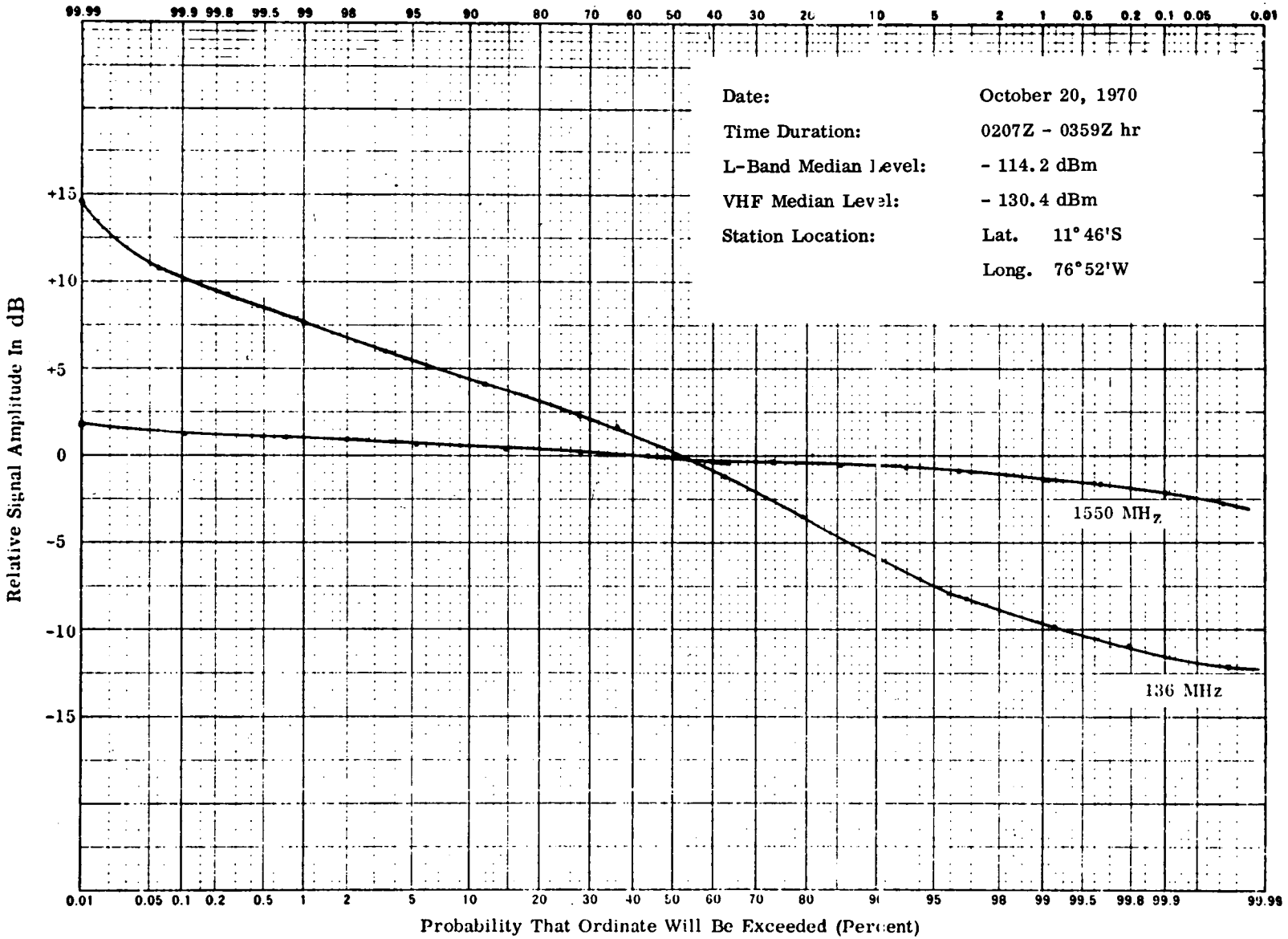

Figure 6. Cumulative Amplitude Distribution of ATS-5 and INTELSAT-I Signals

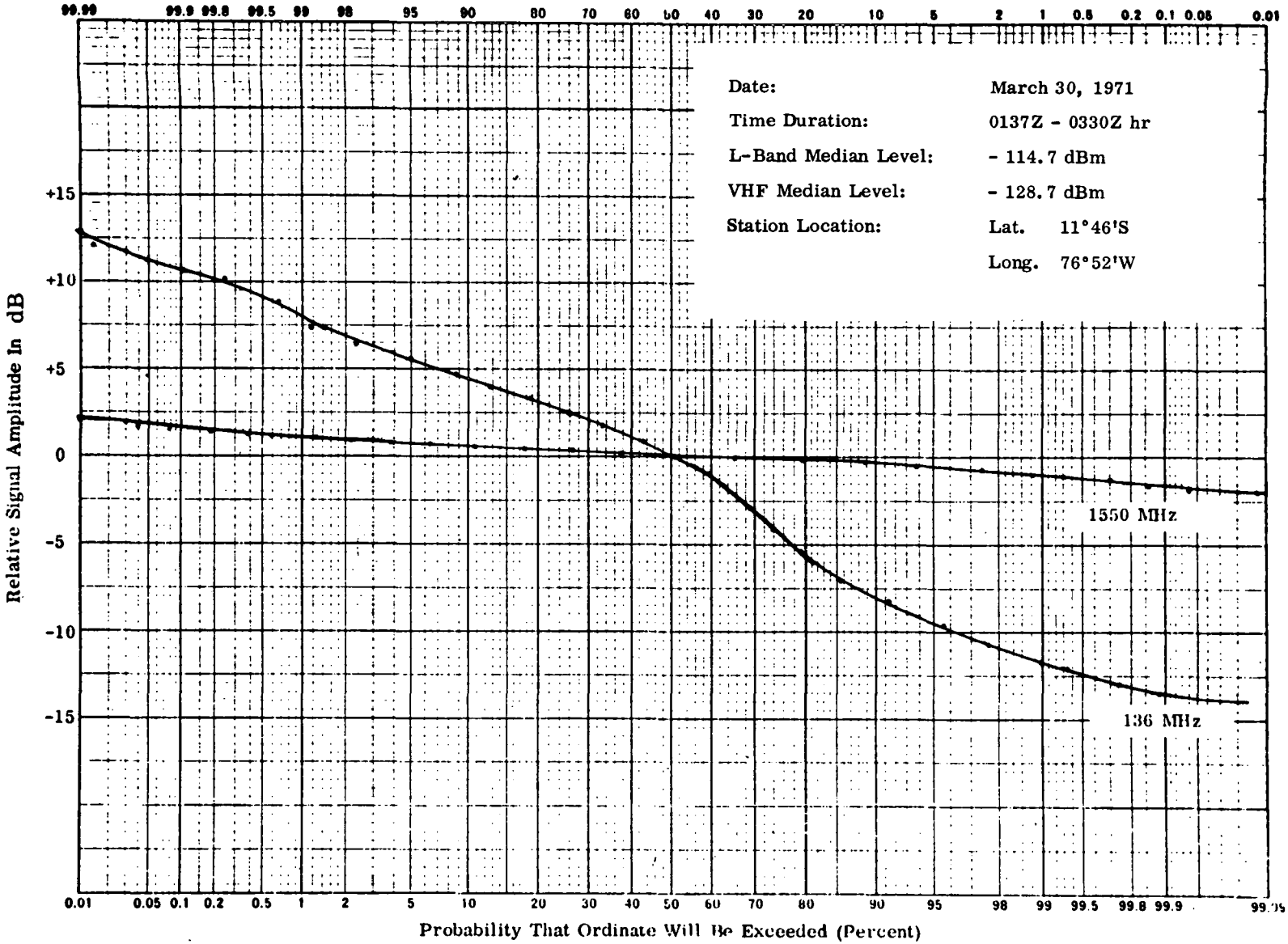

Figure 7. Cumulative Amplitude Distribution of ATS-5 Signals

ACKNOWLEDGMENTS

The contents of this report are results of the efforts of several people. I wish to express my gratitude to those who contributed. I am particularly grateful to Thomas S. Golden, GSFC, for providing the opportunity for me to do this work, and for his invaluable guidance and assistance. To the personnel of the Institute Geofisco del Peru, I am grateful for their contribution in conducting this experiment. A note of thanks is also expressed to Thomas J. Karras, GSFC, for his assistance and cooperation in digitizing the analog tapes, and to J. Piazza, Westinghouse Electric Corporation, for the development of the computer programs used to process the data.

REFERENCES

1. Golden, T. S. "Ionospheric Distortion of Minitrack Signals in South America." GSFC X-525-68-54. February 1968

2. Aarons, J.; Allen, T. J.; Mullen, J. P.; Whitney, H. E.; Elkins, T. J.; and Klobuchar, J. A. "A Survey of Scintillation Data and its Relationship to Satellite Communications." Radio Astronomy Branch. Air Force Cambridge Research Laboratory. August 1969

3. Piazza, J. L., Fisher, H. B., and Johnson, C. D. "A Process for Reduction of Experimental Scintillation Statistics Using Computer Techniques." Westinghouse Electric Corporation. Defense and Space Center. September 1971

APPENDIX A

(Figures A-1 and A-2)

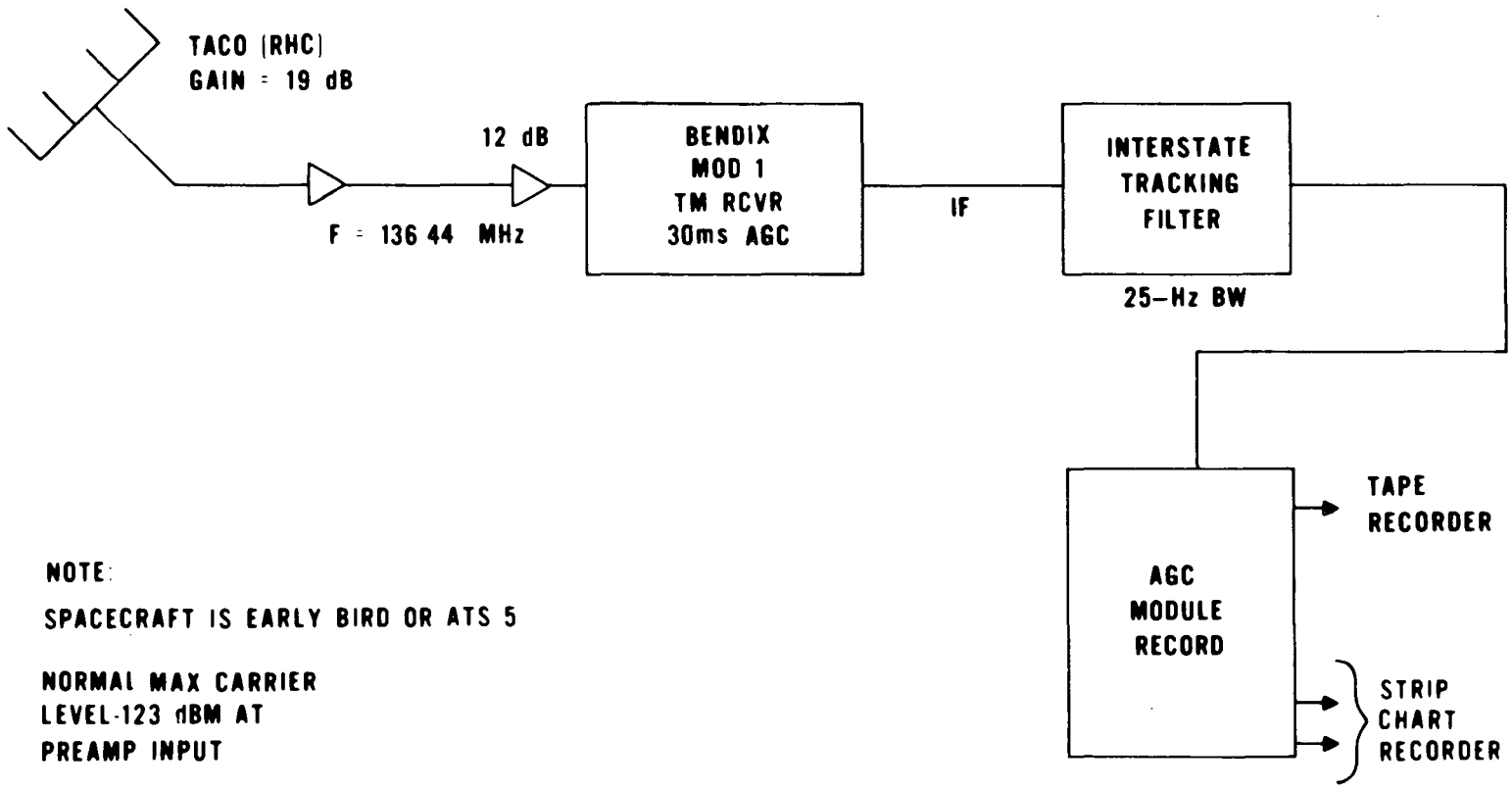

Figure A-1. VHF Ground-Station Test Configuration

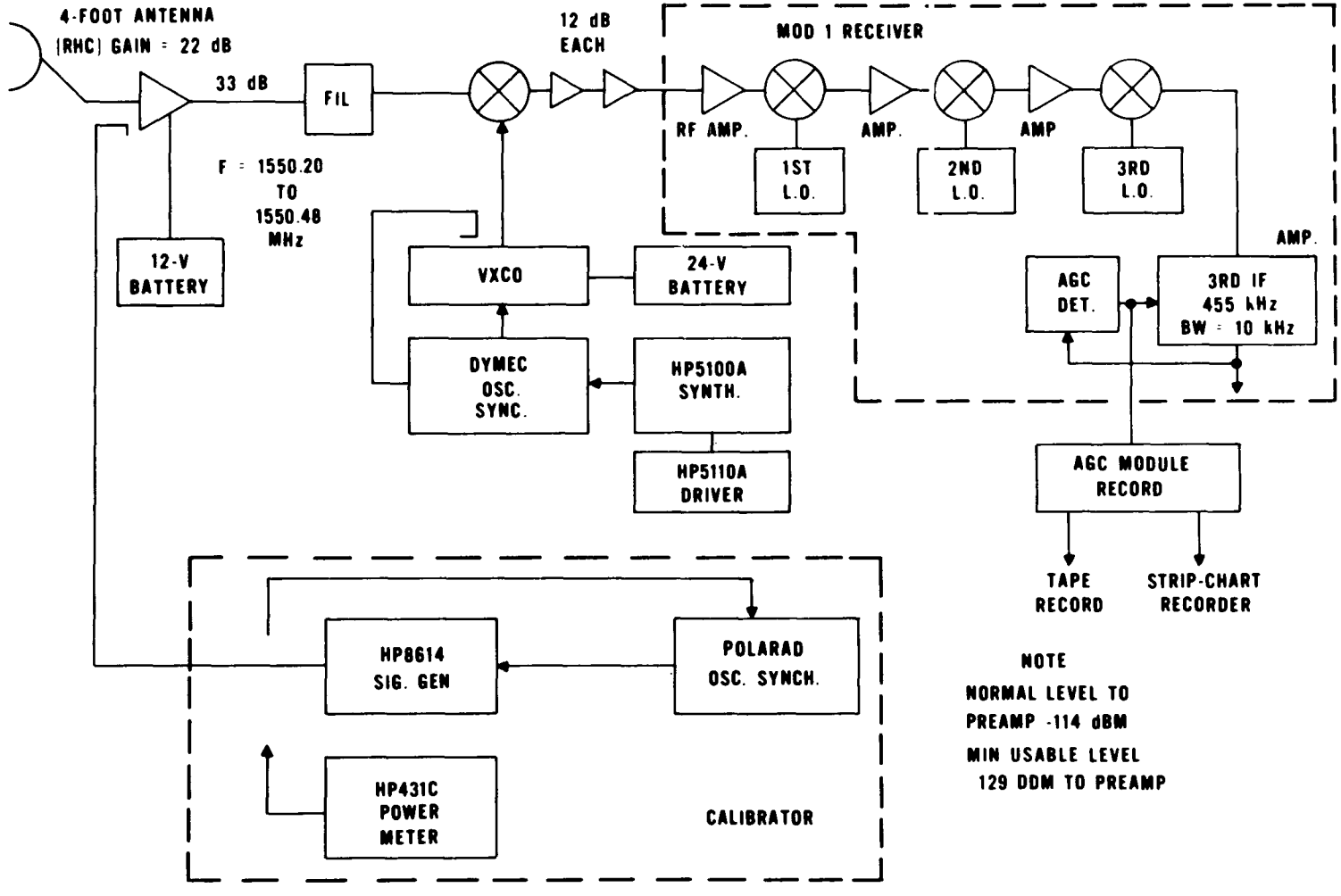

Figure A-2. L-Band Ground-Station Test Configuration

APPENDIX B

Figures B-1 through B-20 show the cumulative amplitude distribution of ATS-5 and INTELSAT-I signals for certain days from October 2, 1970 through October 21, 1970. Figures B-21 through B-29 show the cumulative amplitude distribution of ATS-5 signals for certain days from March 15, 1971 through April 8, 1971.

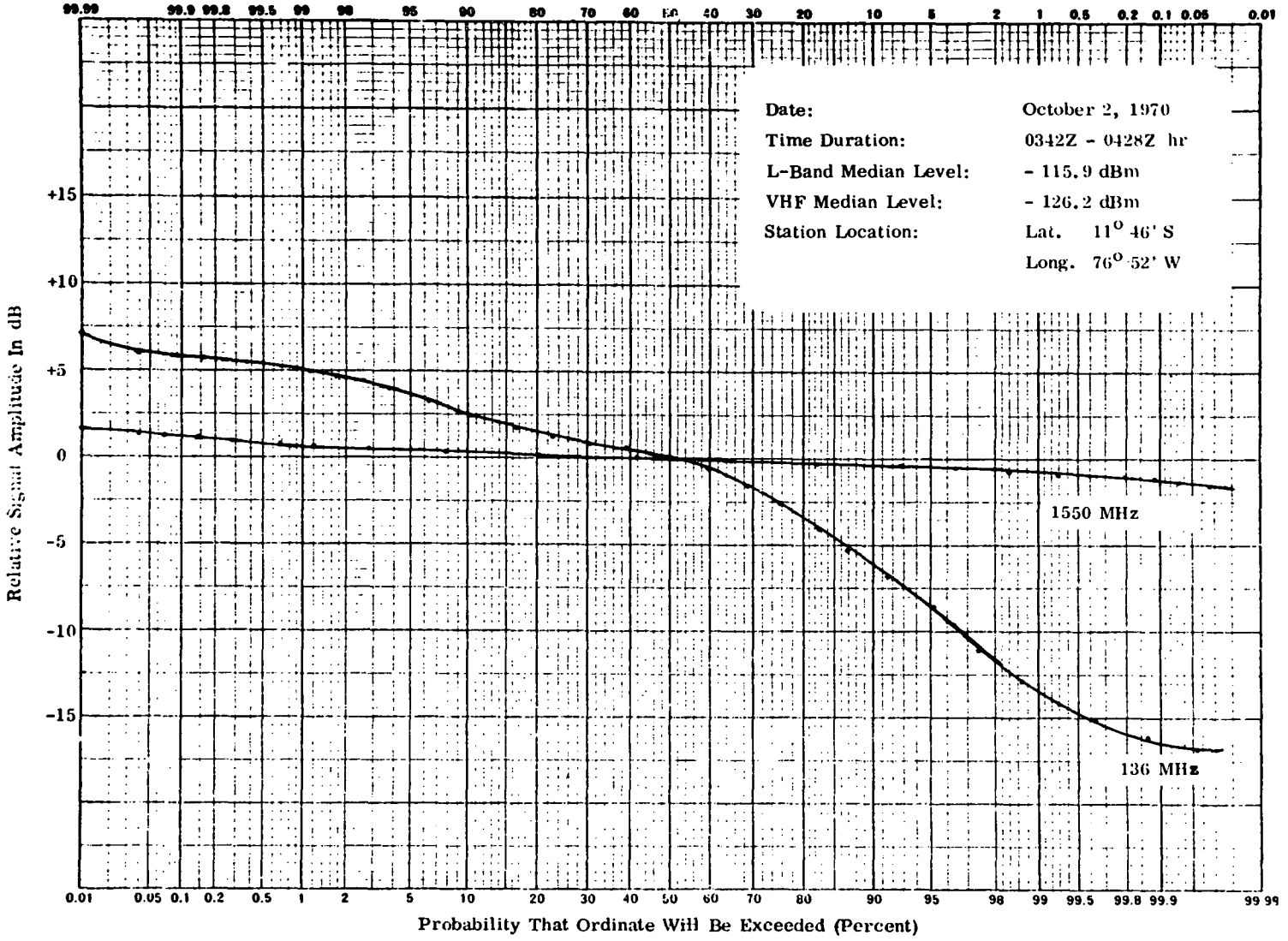

Figure B-1. Cumulative Amplitude Distribution of ATS-5 And INTELSAT-I Signals, 0342Z-0428Z Hours

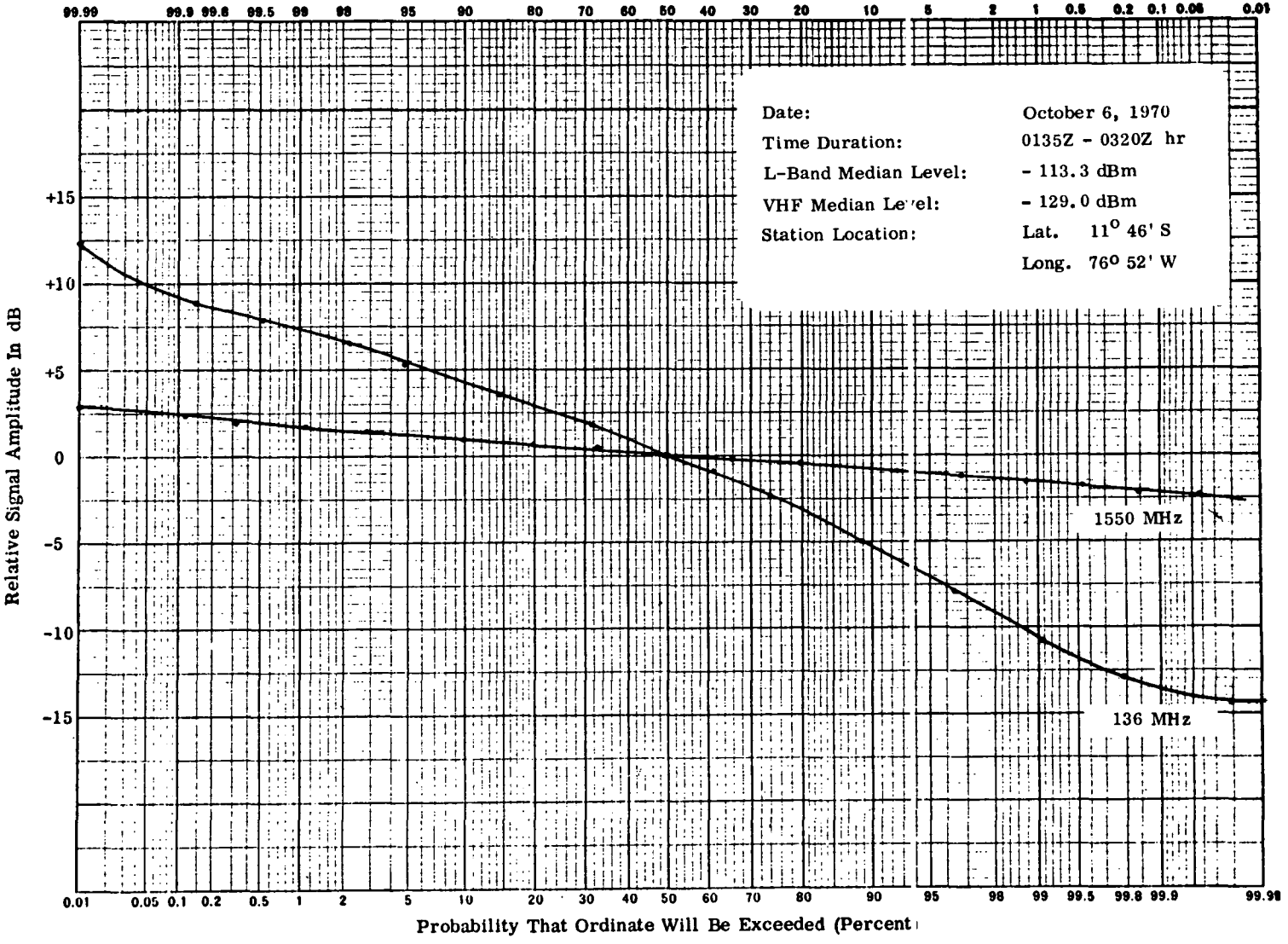

Figure B-2. Cumulative Amplitude Distribution of ATS-5 And INTELSAT-I Signals

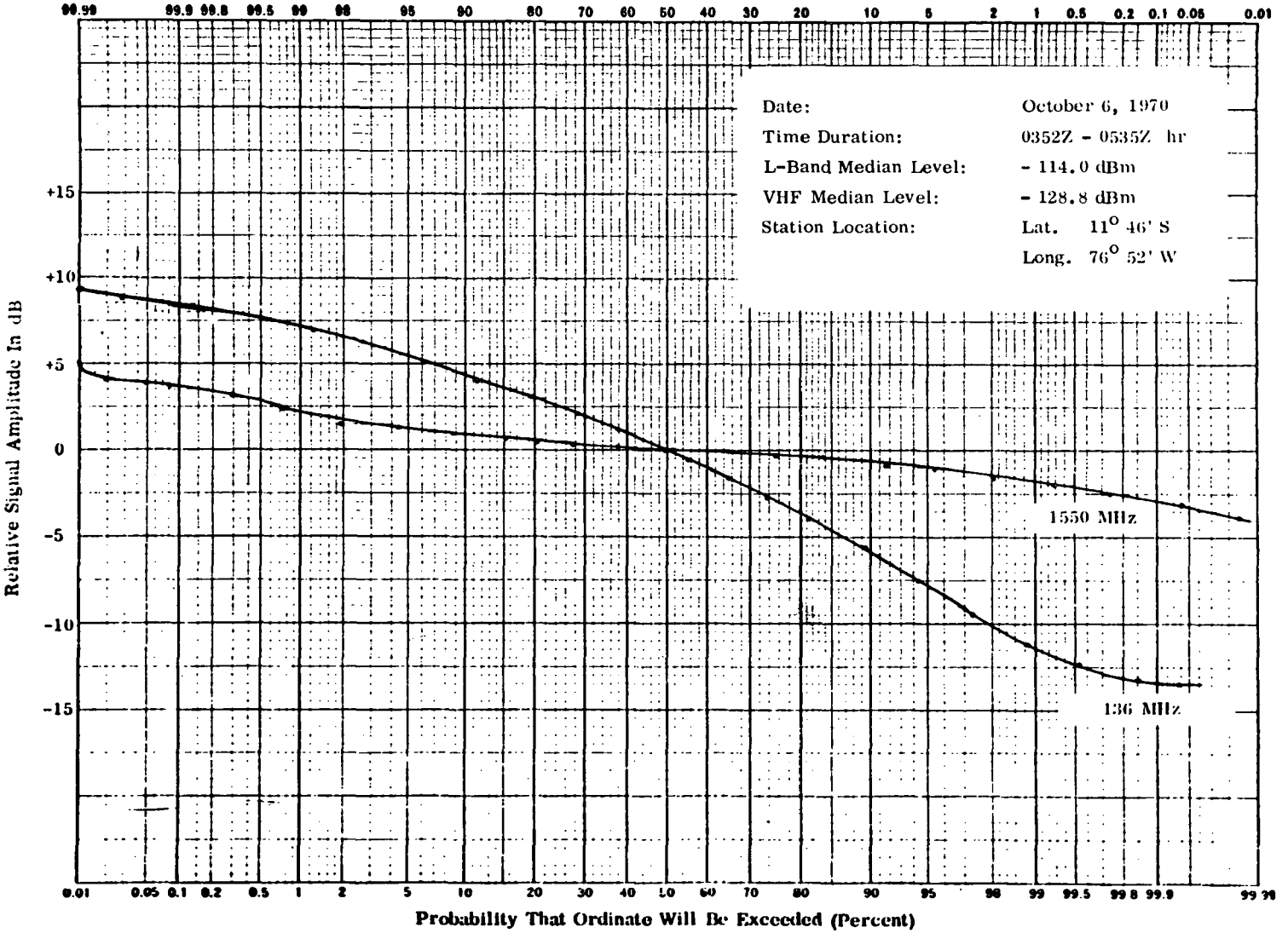

Figure B-3. Cumulative Amplitude Distribution of ATS-5 And INTELSAT-I Signals

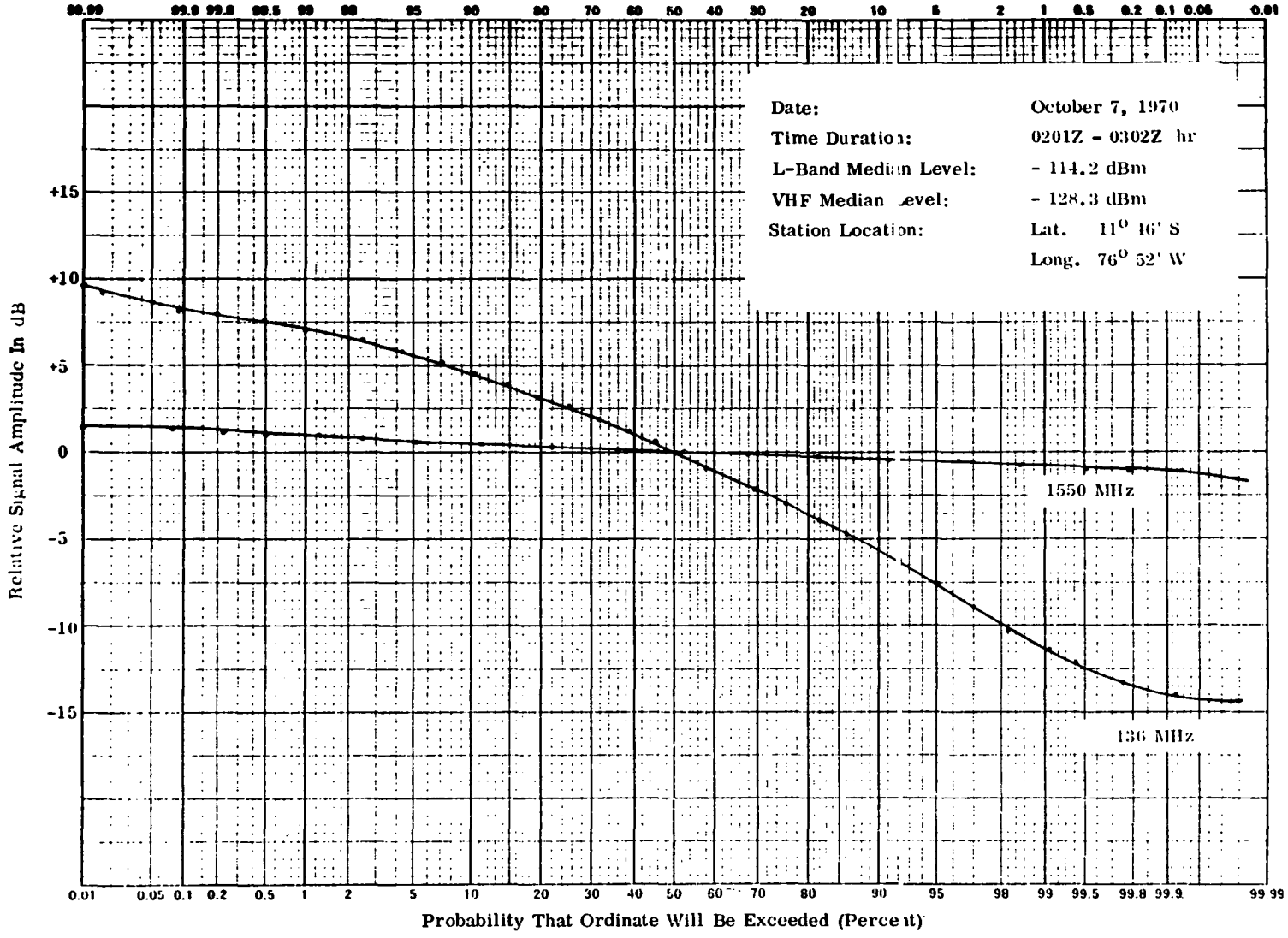

Figure B-4. Cumulative Amplitude Distribution of ATS-5 And INTELSAT-I Signals

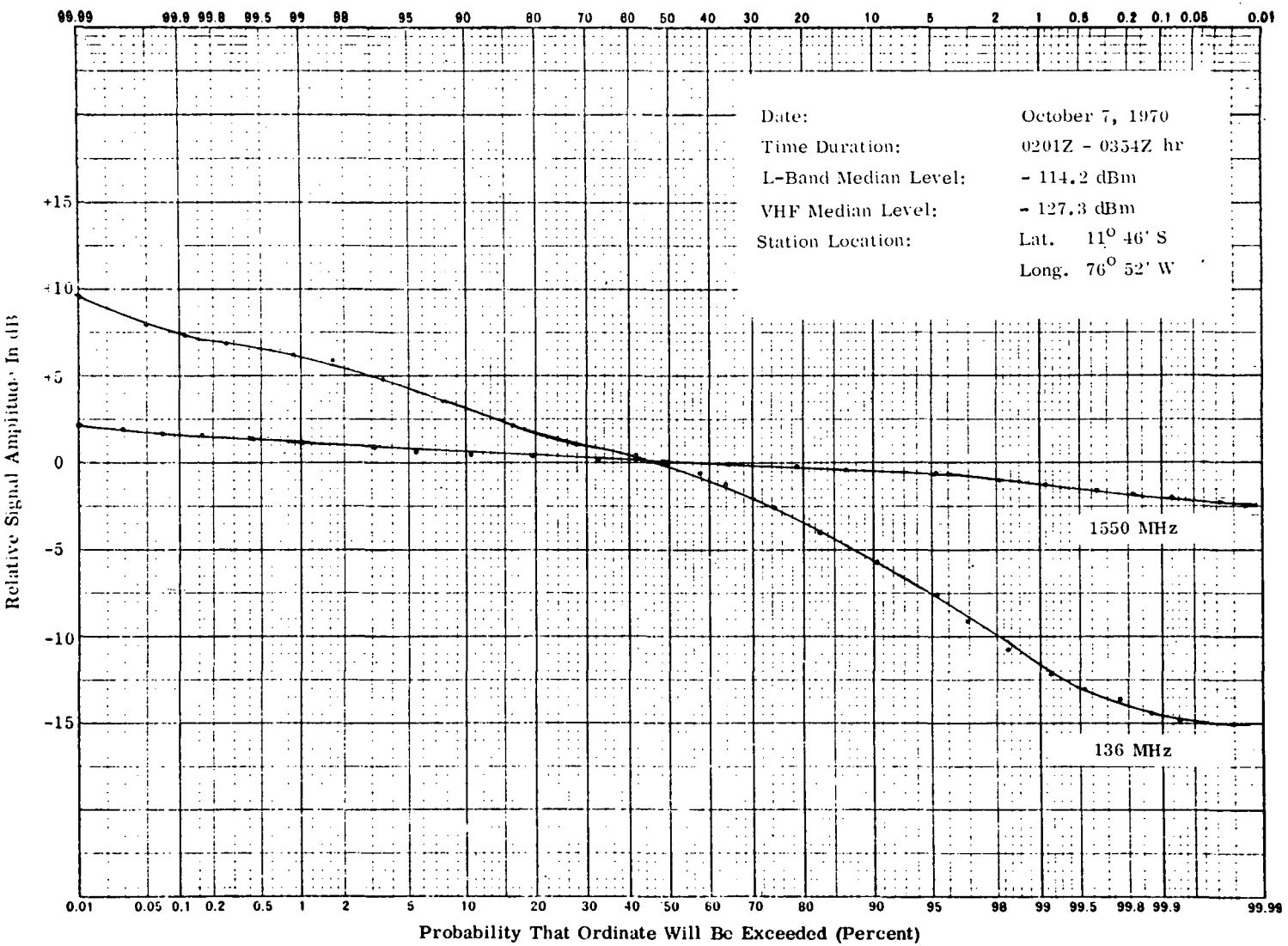

Figure B-5. Cumulative Amplitude Distribution of ATS-5 And INTELSAT-I Signals

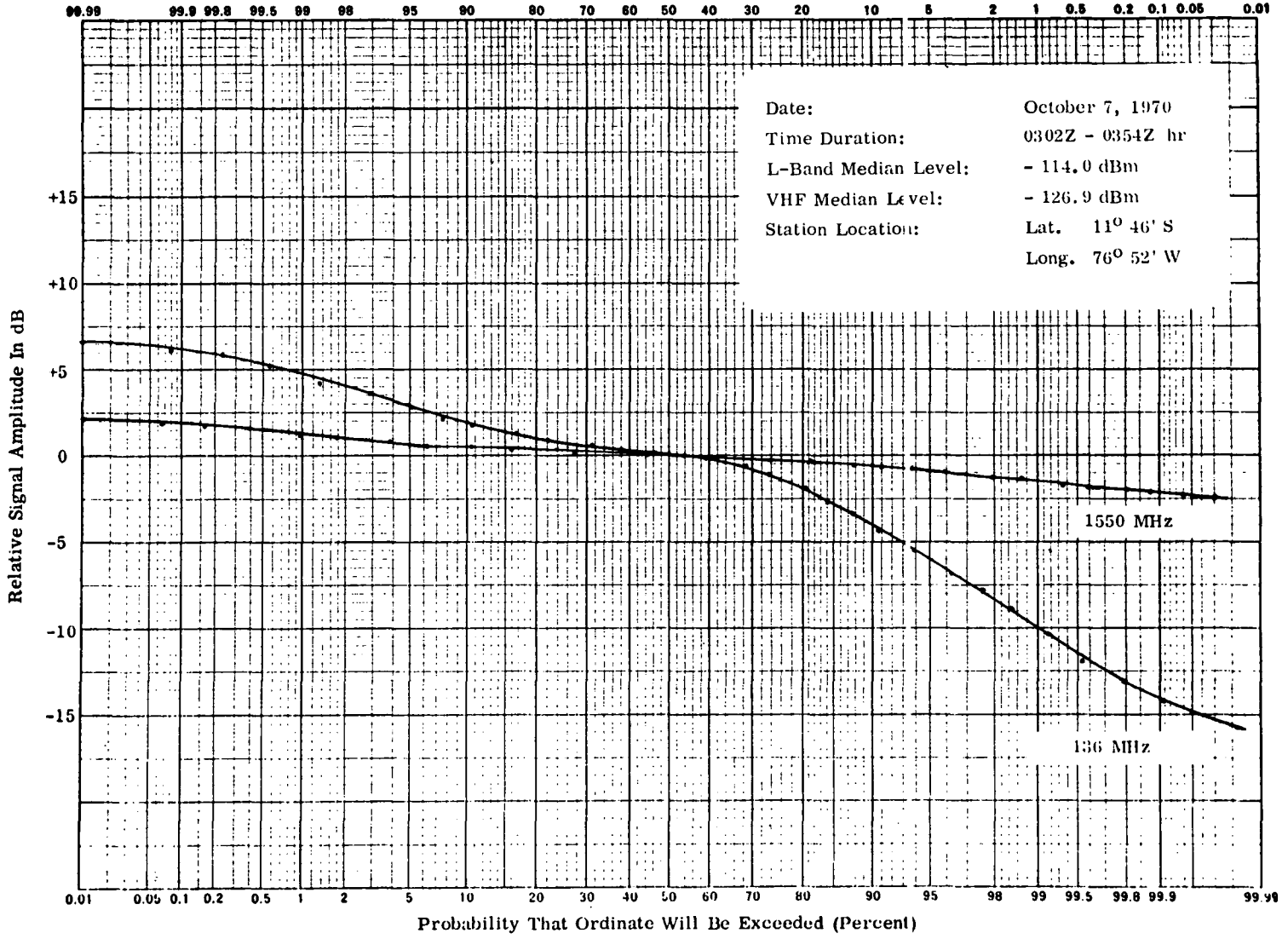

Figure B-6. Cumulative Amplitude Distribution of ATS-5 And INTELSAT-I Signals

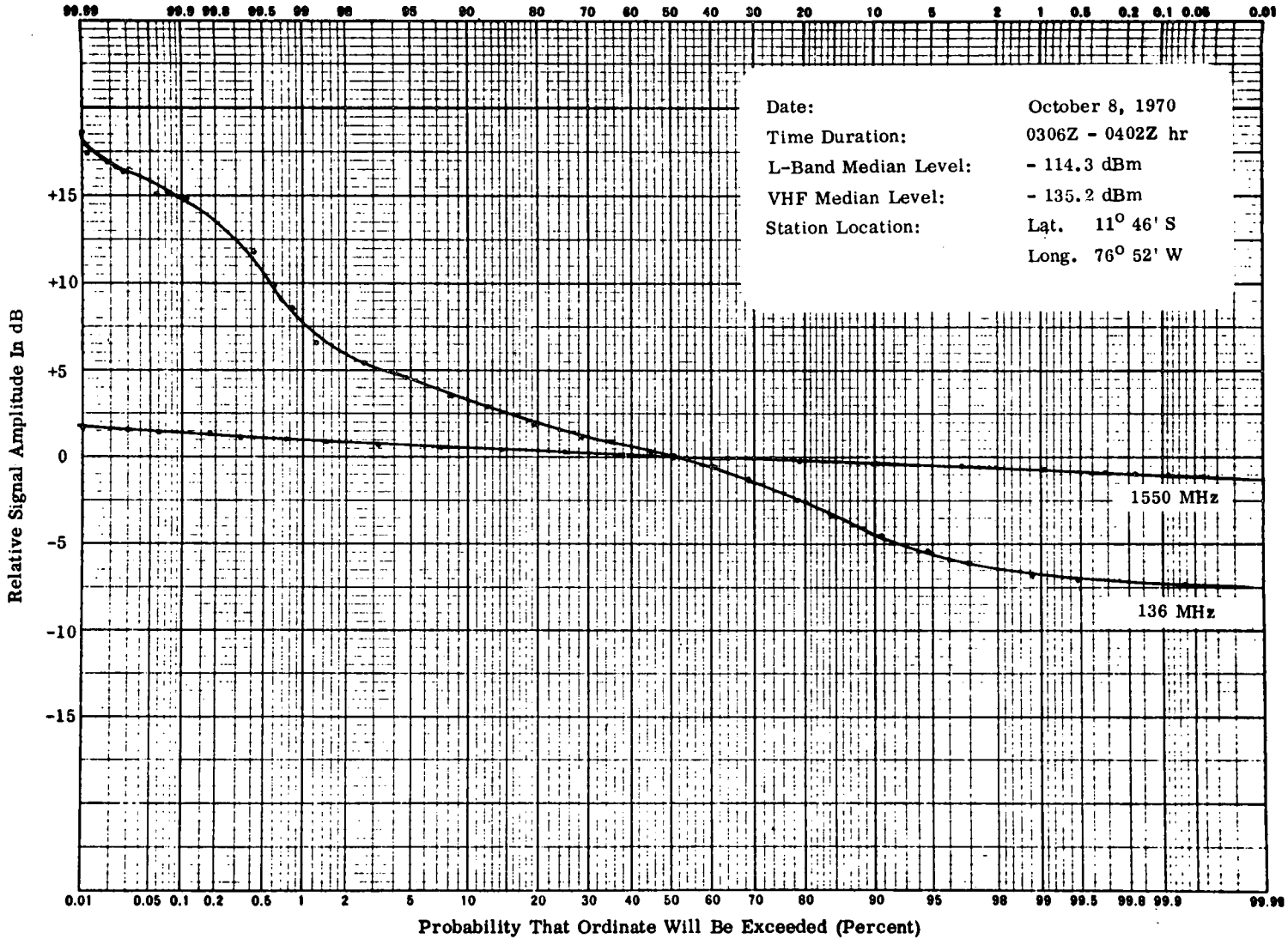

Figure B-7. Cumulative Amplitude Distribution of ATS-5 And INTELSAT-I Signals

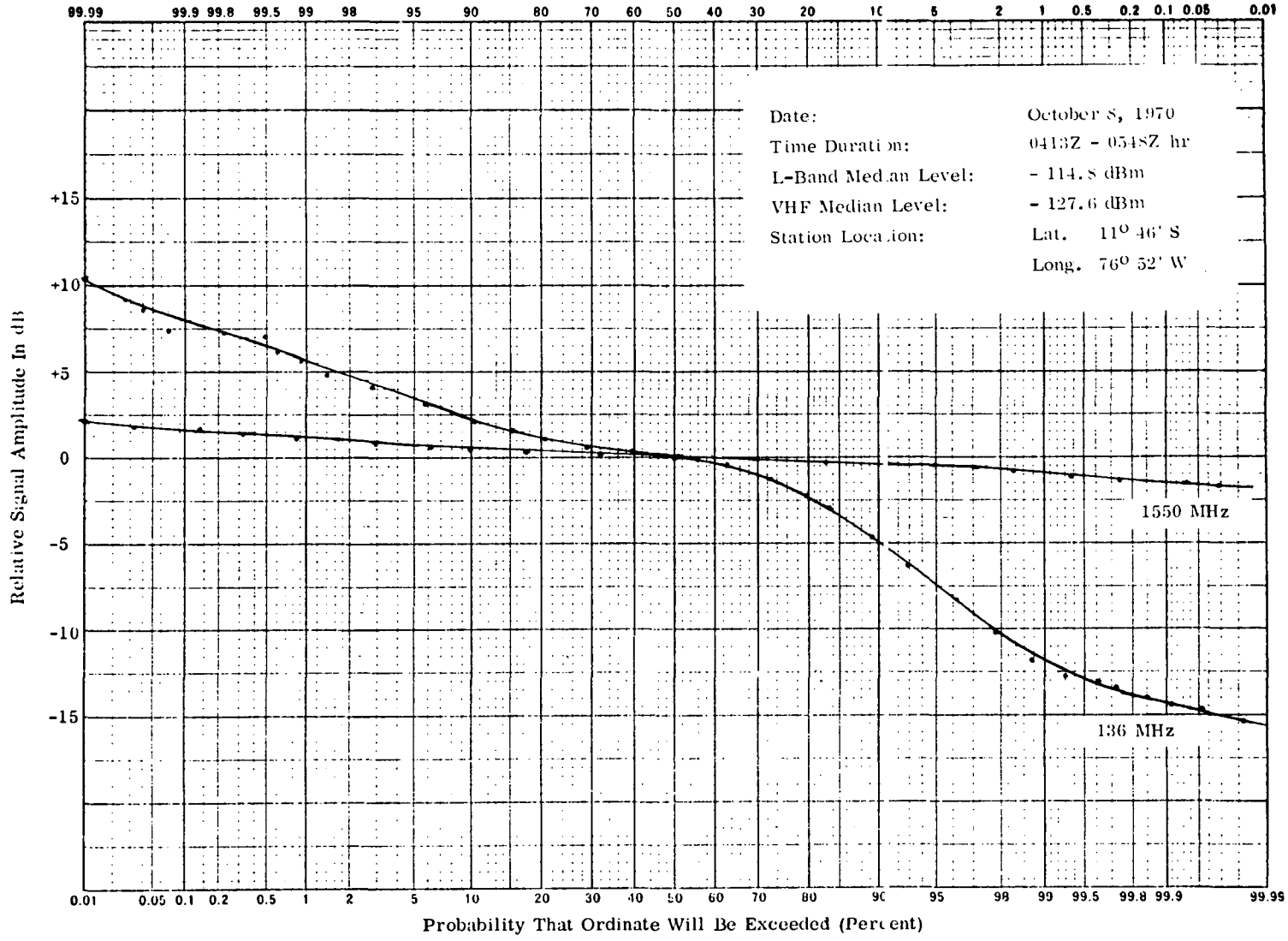

Figure B-8. Cumulative Amplitude Distribution of ATS-5 And INTELSAT-I Signals

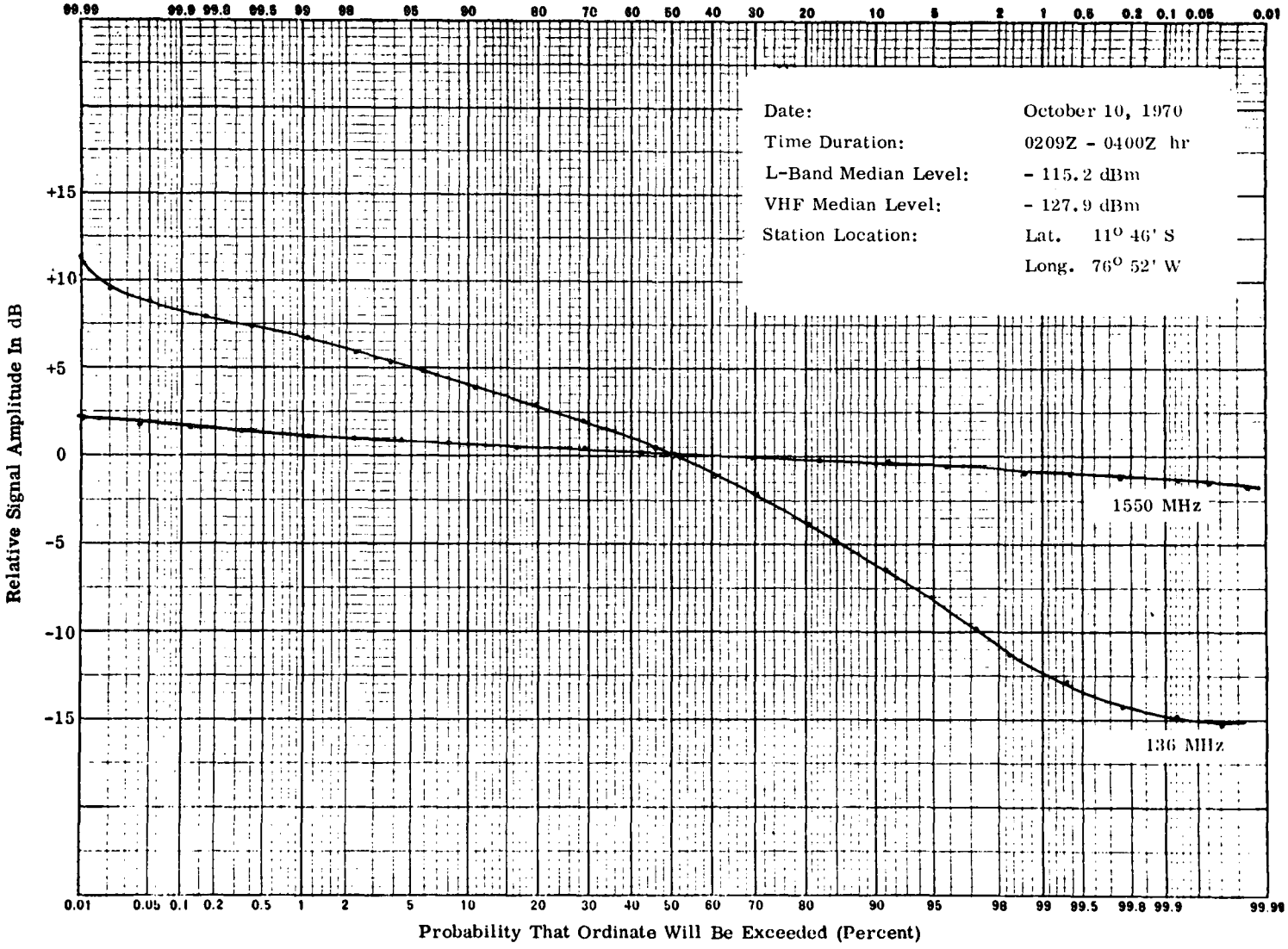

Figure B-9. Cumulative Amplitude Distribution of ATS-5 And INTELSAT-I Signals

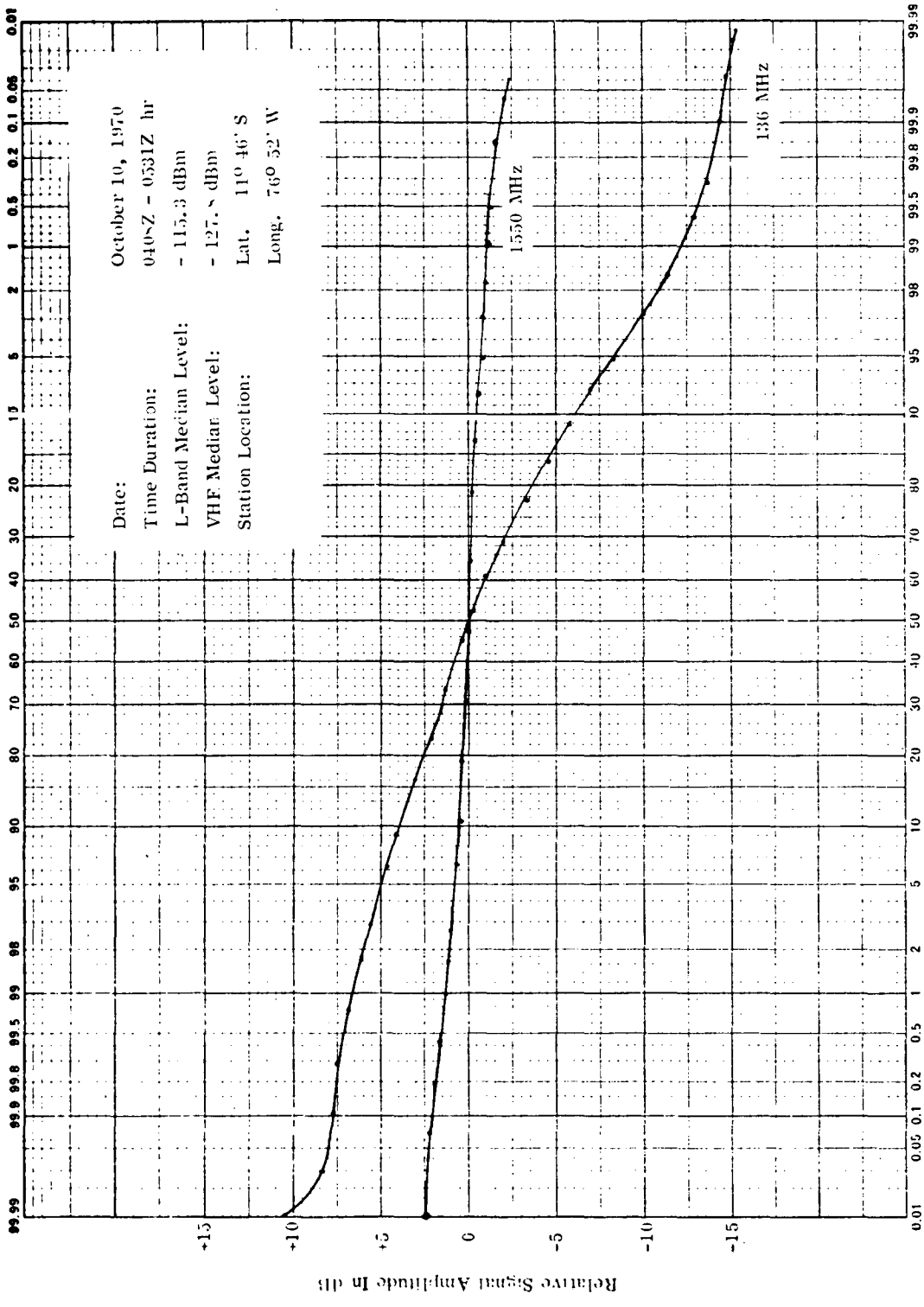

Figure B-10. Cumulative Amplitude Distribution of ATS-5 And INTELSAT-I Signals

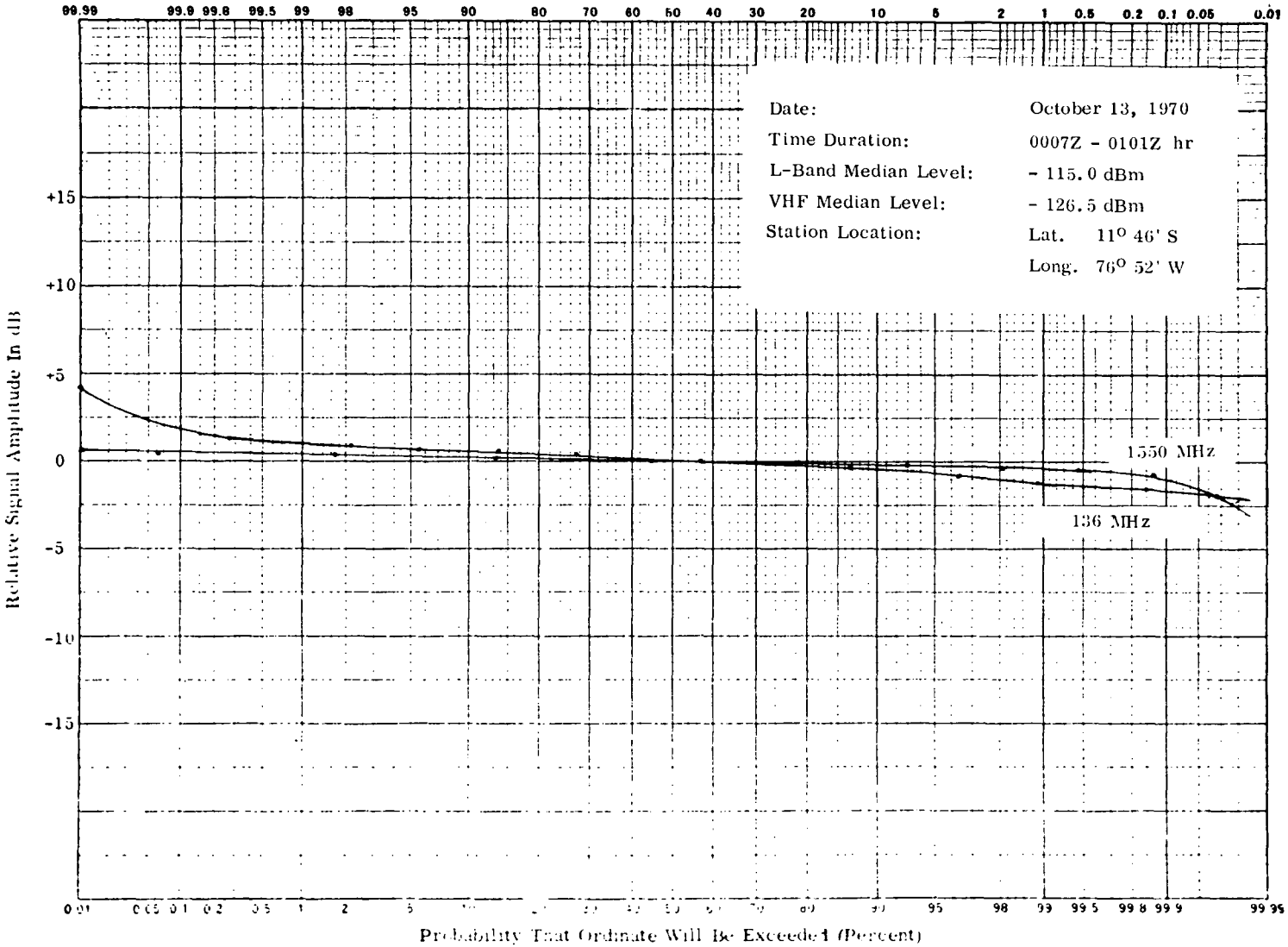

Figure B-11. Cumulative Amplitude Distribution of ATS-5 And INTELSAT-I Signals

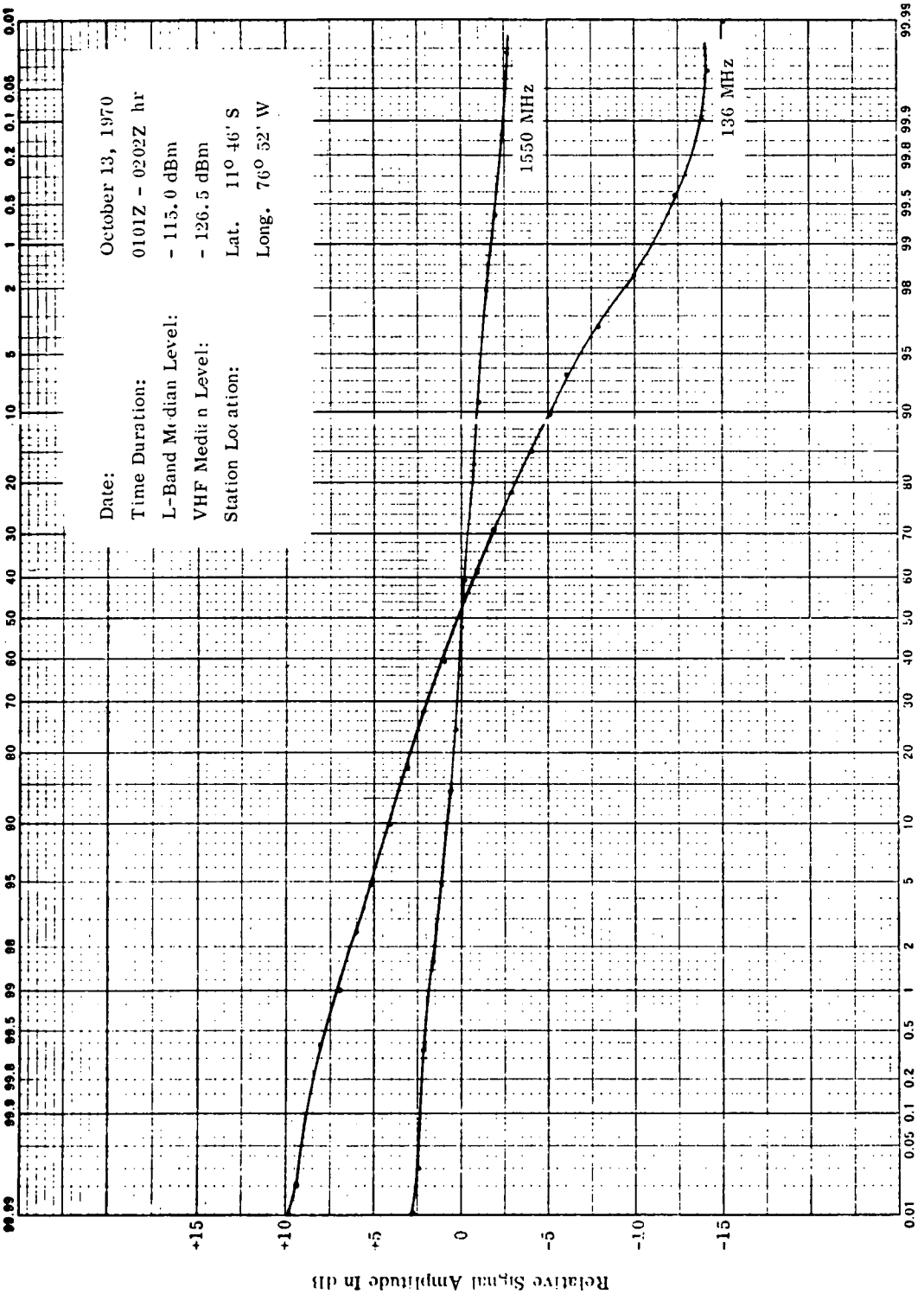

Figure B-12. Cumulative Amplitude Distribution of ATS-5 And INTELSAT-I Signals

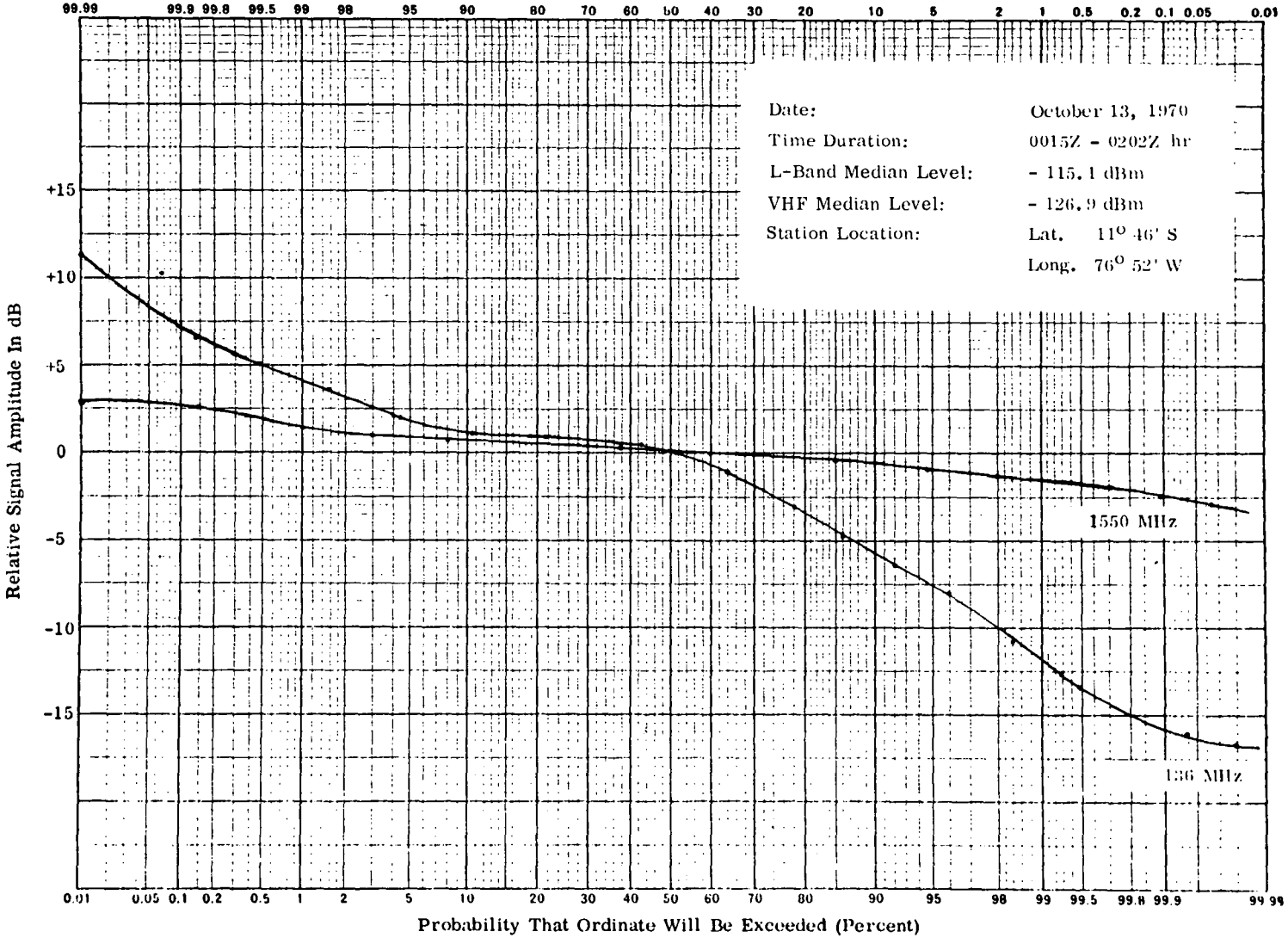

Figure B-13. Cumulative Amplitude Distribution of ATS-5 And INTELSAT-I Signals

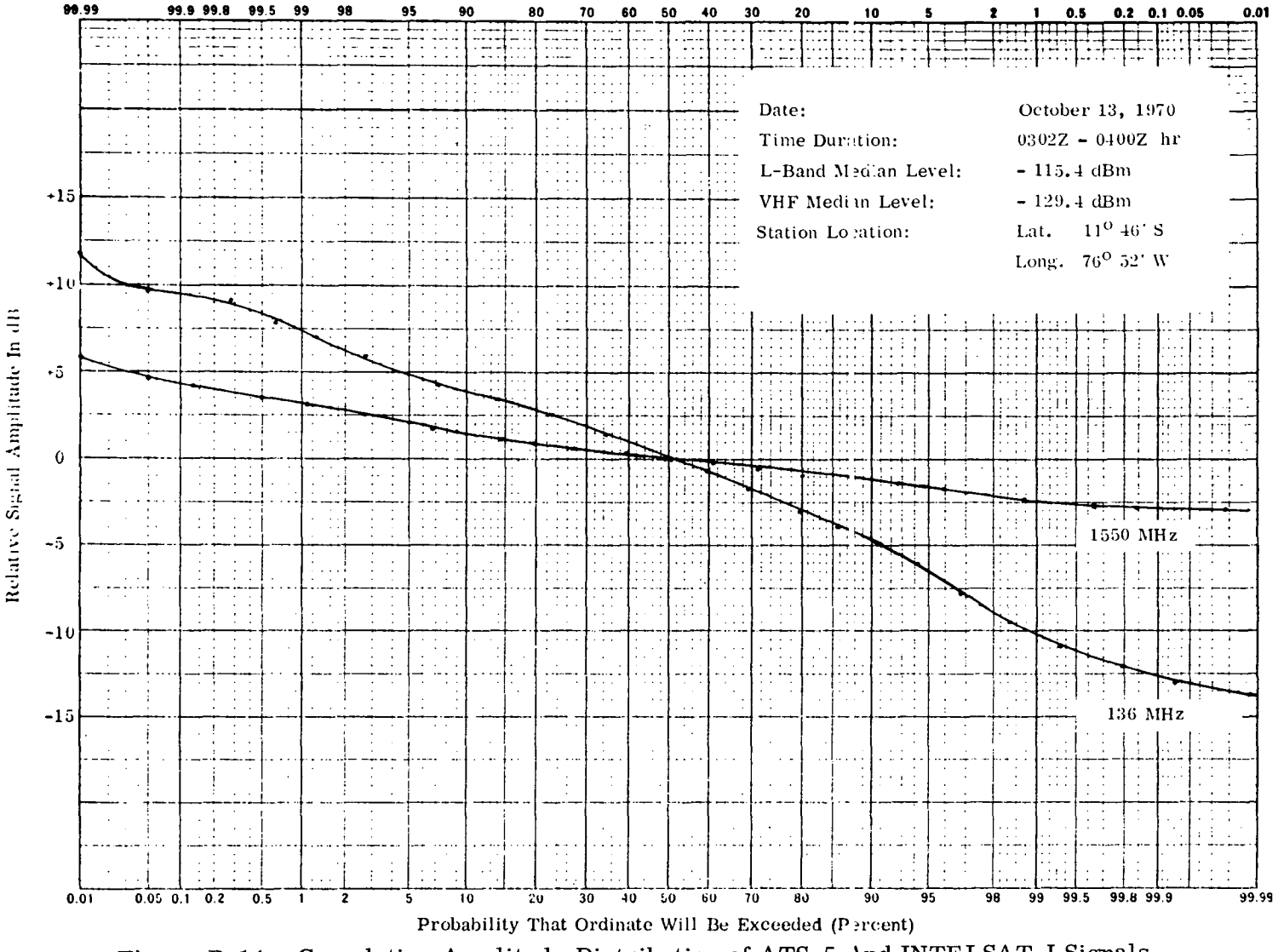

Figure B-14. Cumulative Amplitude Distribution of ATS-5 And INTELSAT-I Signals

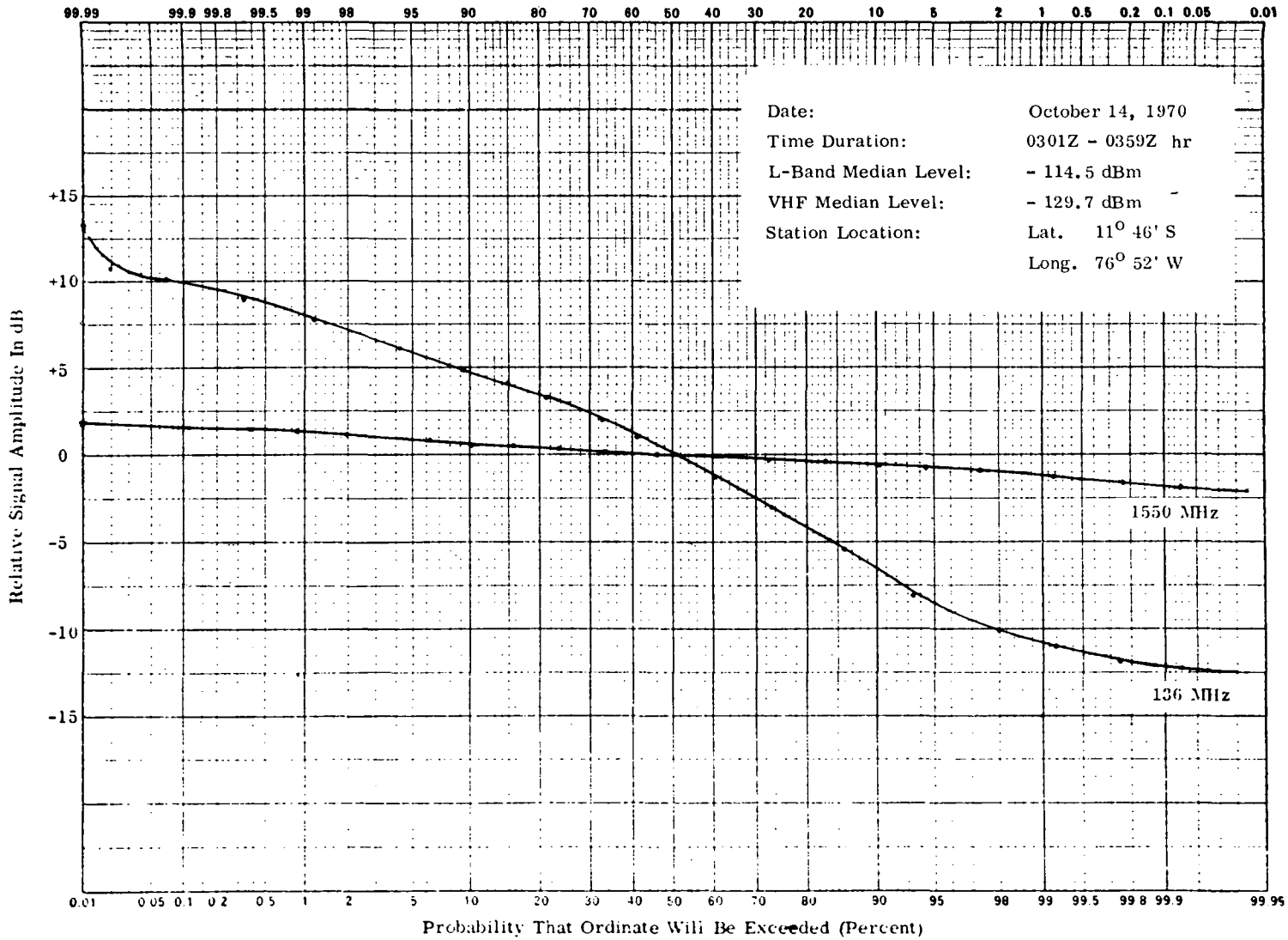

Figure B-15. Cumulative Amplitude Distribution of ATS-5 And INTELSAT-I Signals

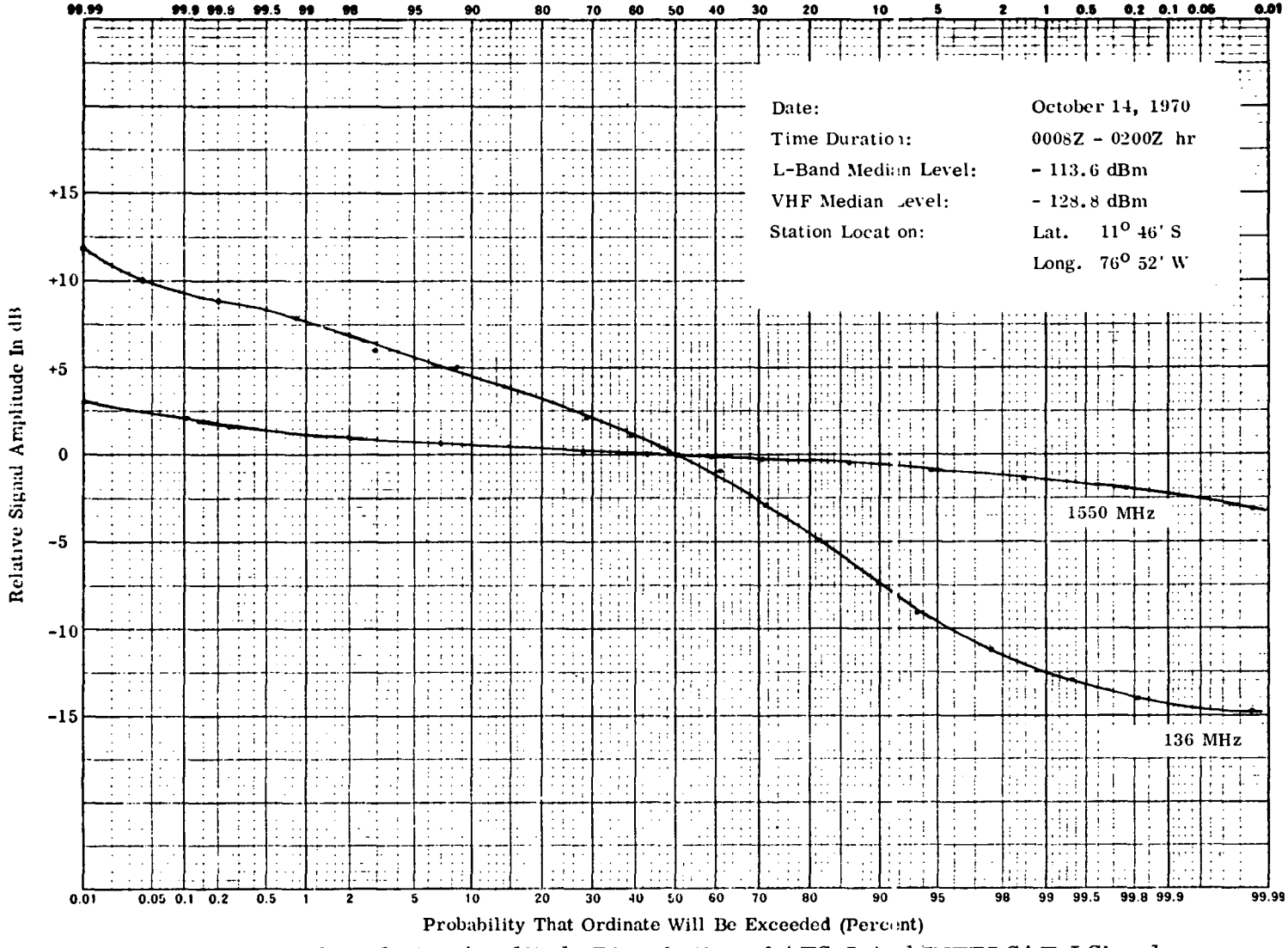

Figure B-16. Cumulative Amplitude Distribution of ATS-5 And INTELSAT-I Signals

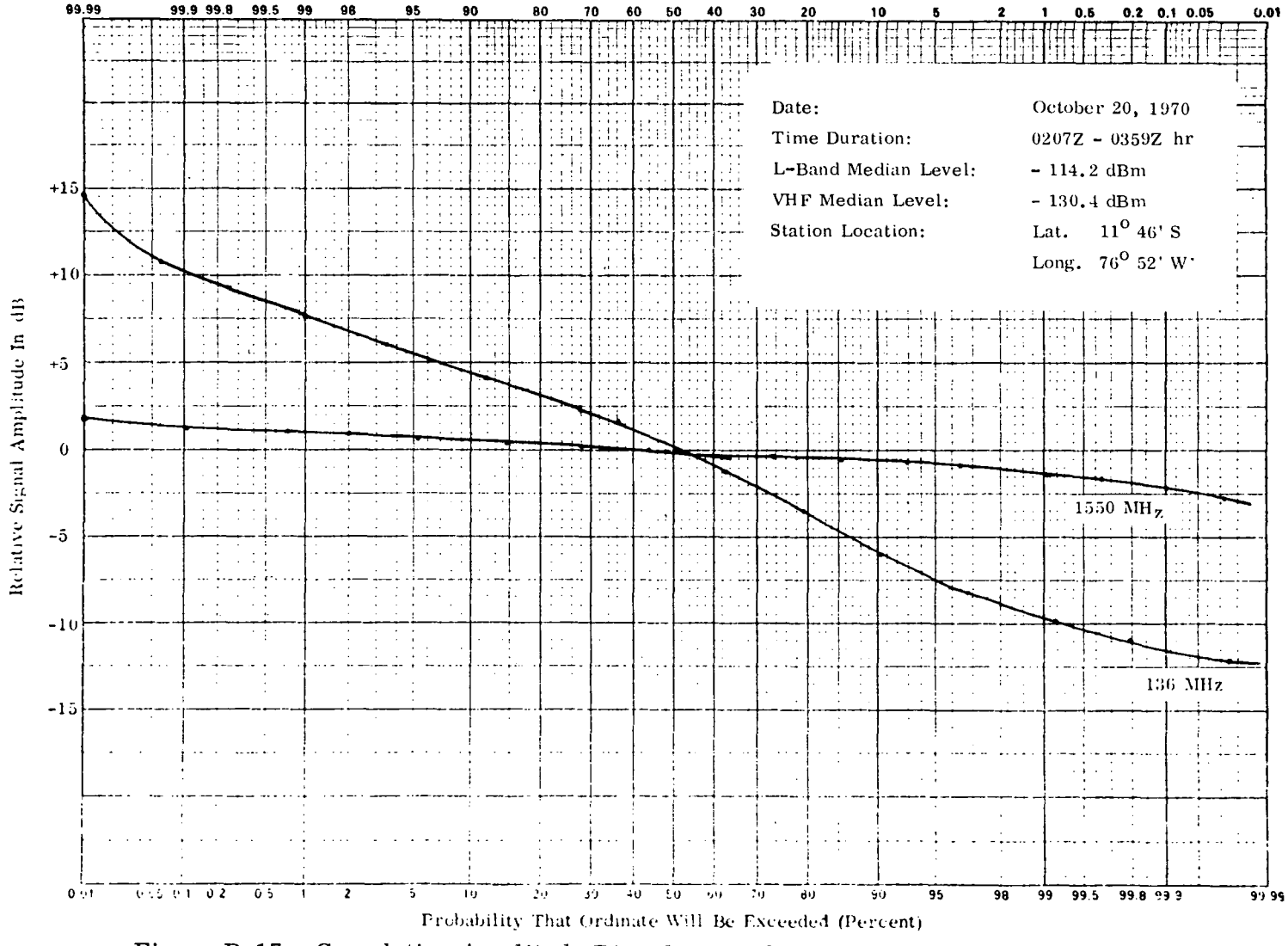

Figure B-17. Cumulative Amplitude Distribution of ATS-5 And INTELSAT-I Signals

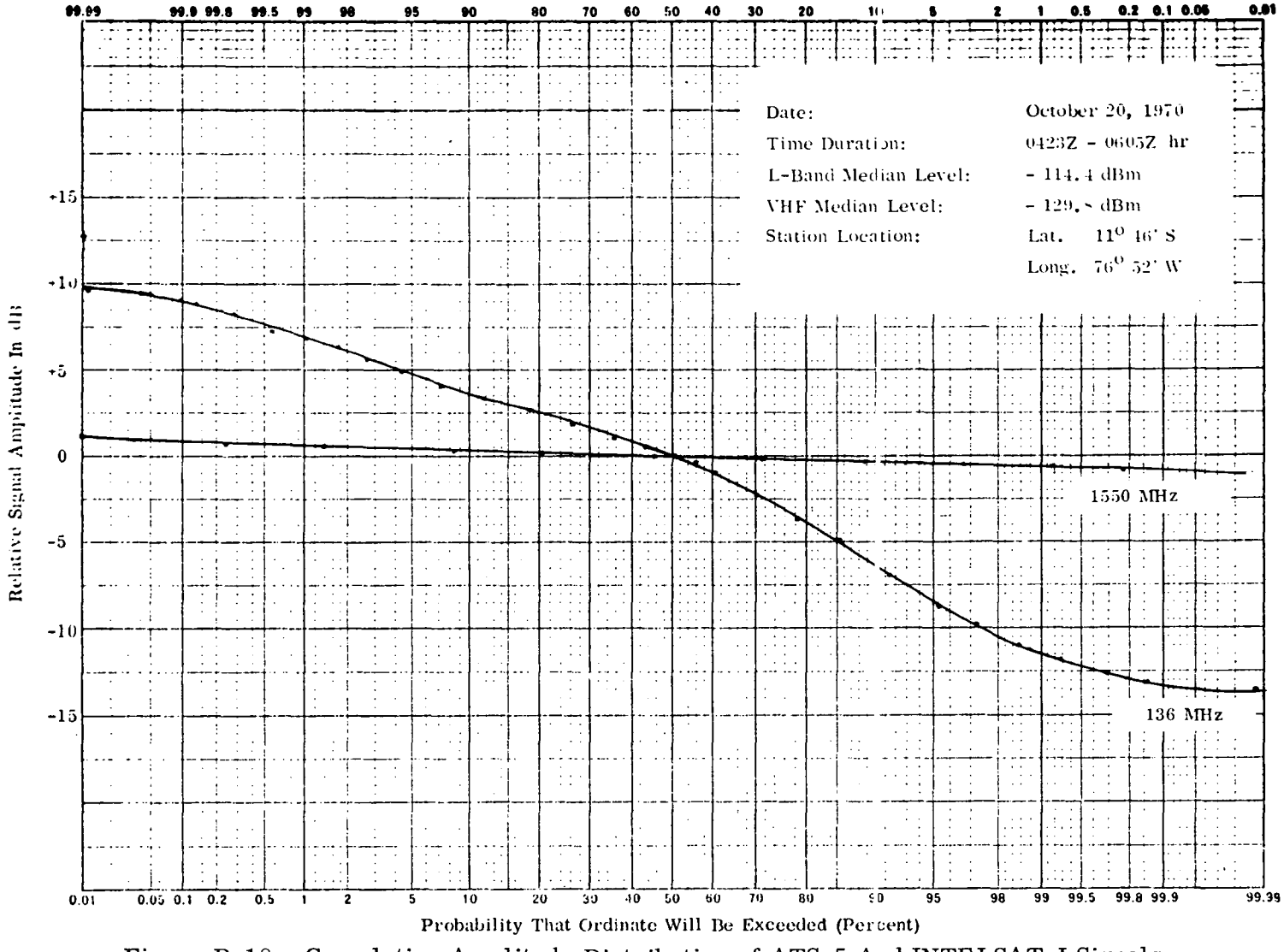

Figure B-18. Cumulative Amplitude Distribution of ATS-5 And INTELSAT-I Signals

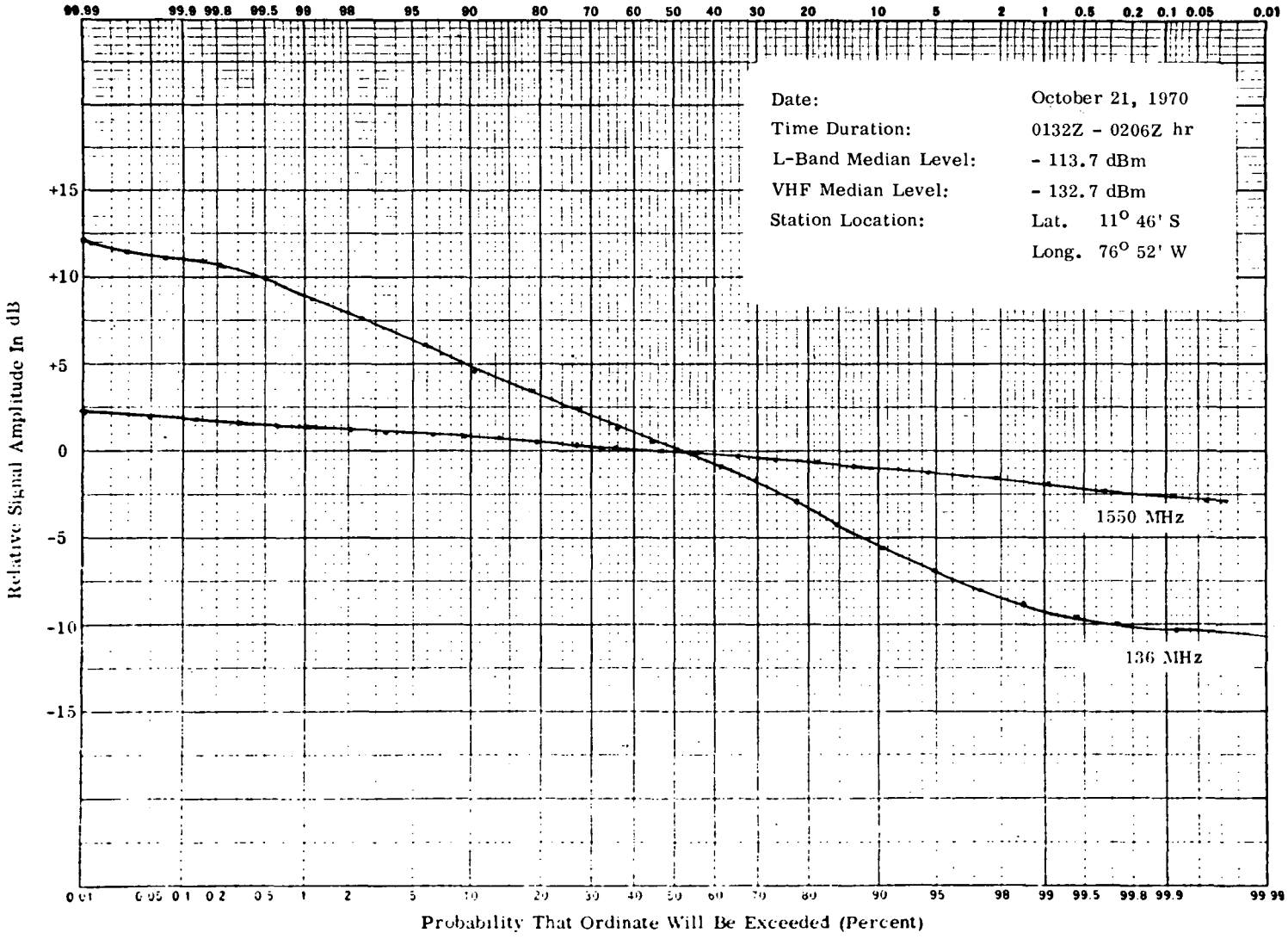

Figure B-19. Cumulative Amplitude Distribution of ATS-5 And INTELSAT-I Signals

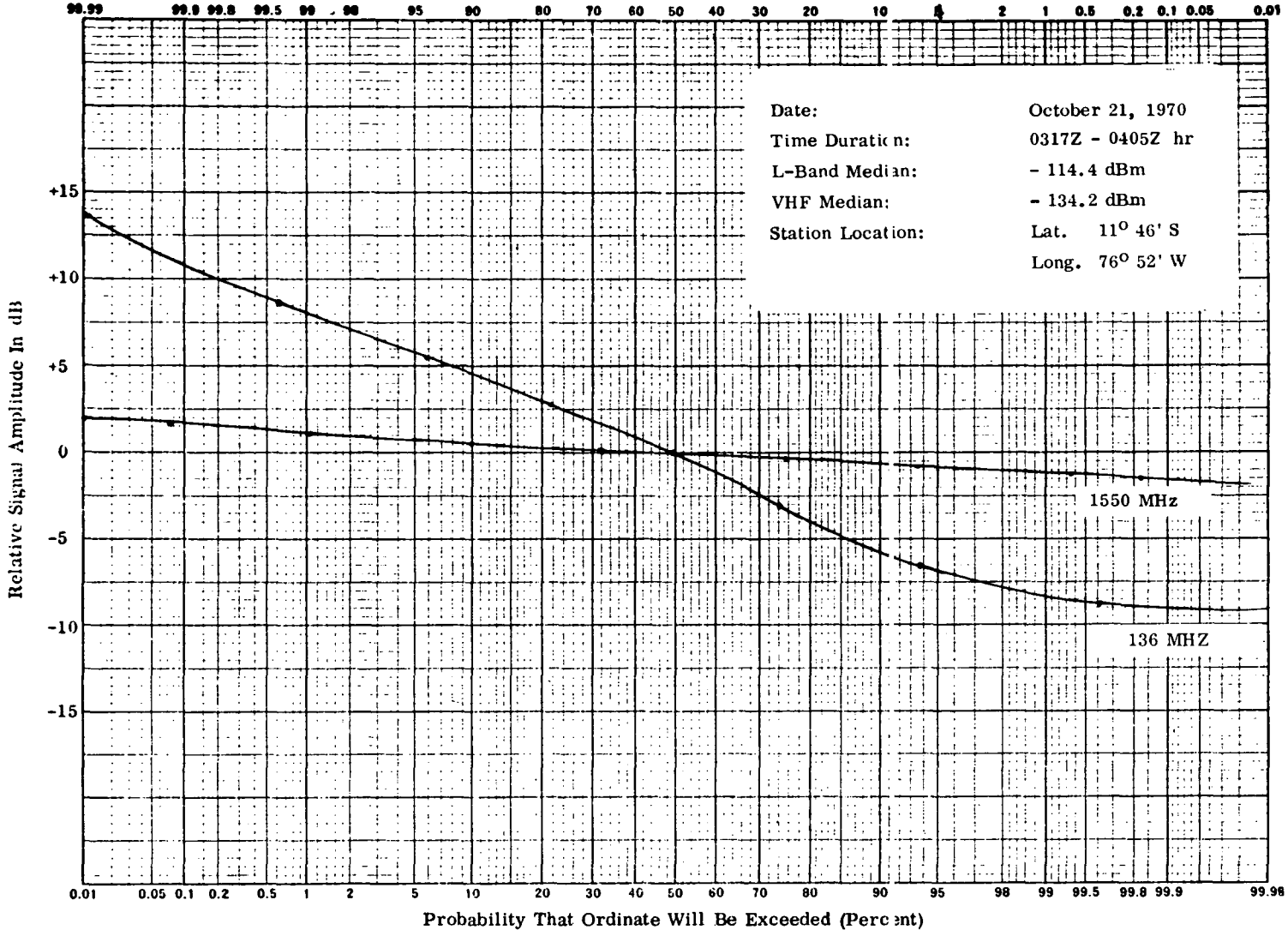

Figure B-20. Cumulative Amplitude Distribution of ATS-5 And INTELSAT-I Signals

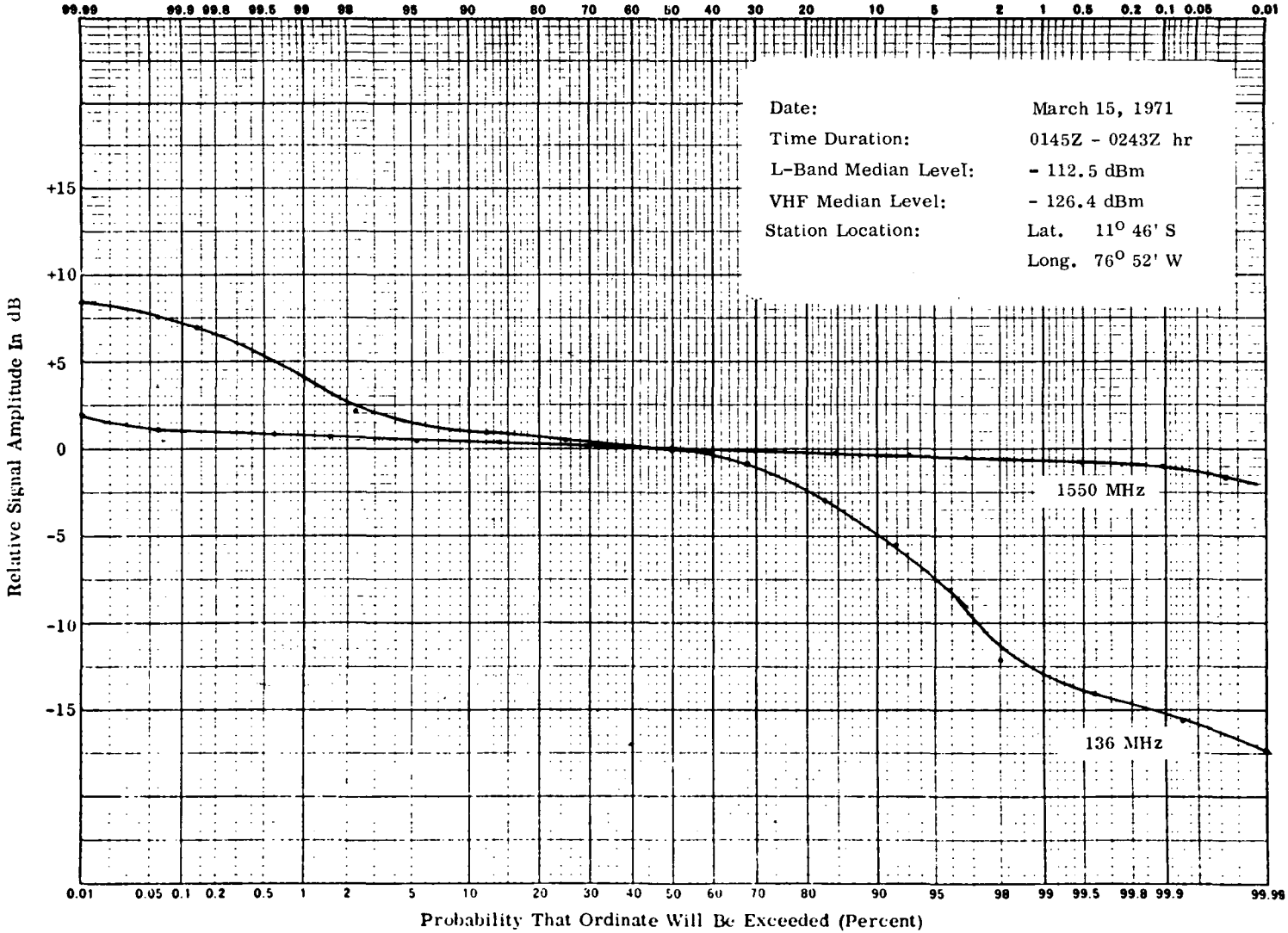

Figure B-21. Cumulative Amplitude Distribution of ATS-5 Signals

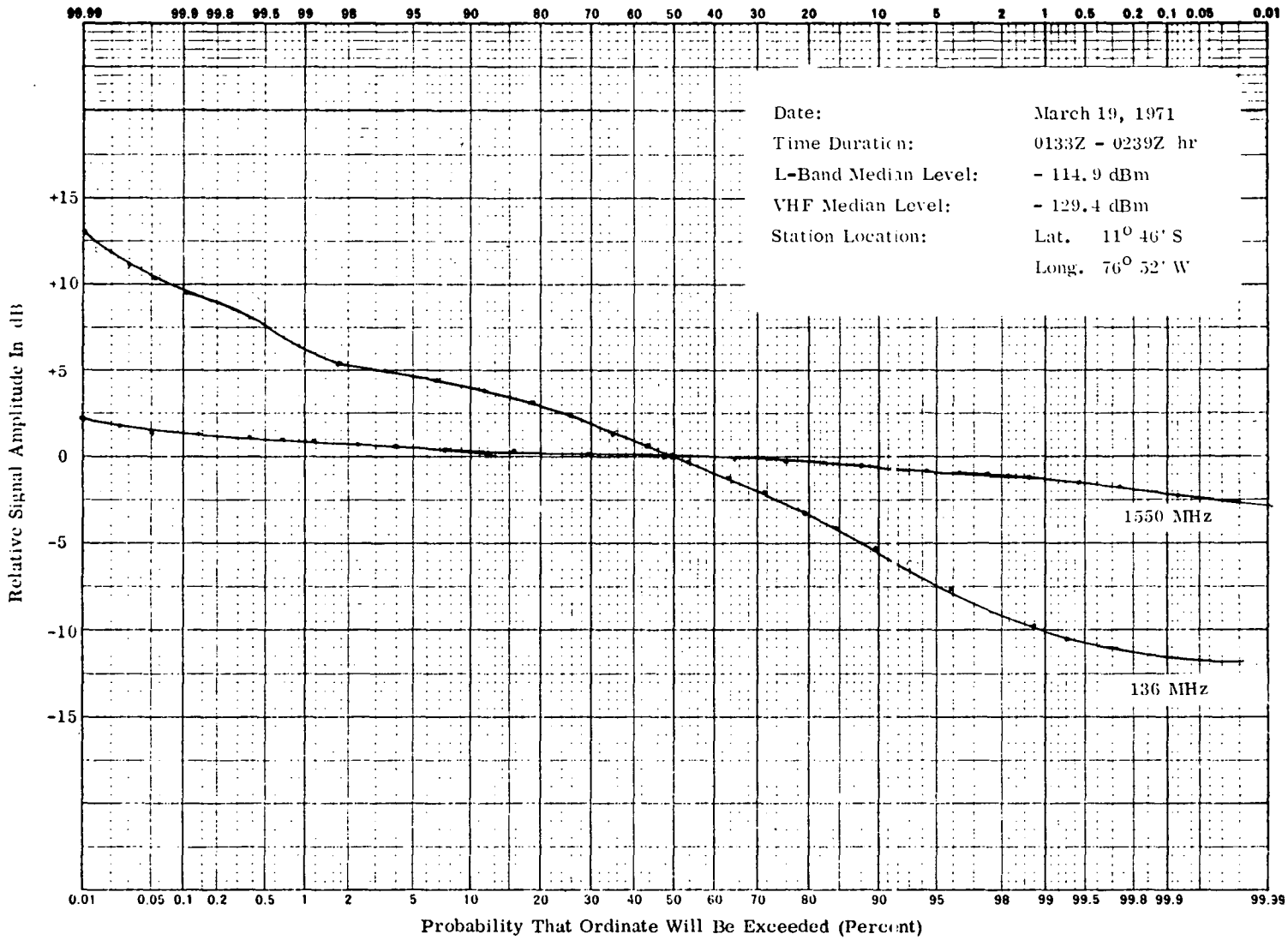

Figure B-22. Cumulative Amplitude Distribution of ATS-5 Signals

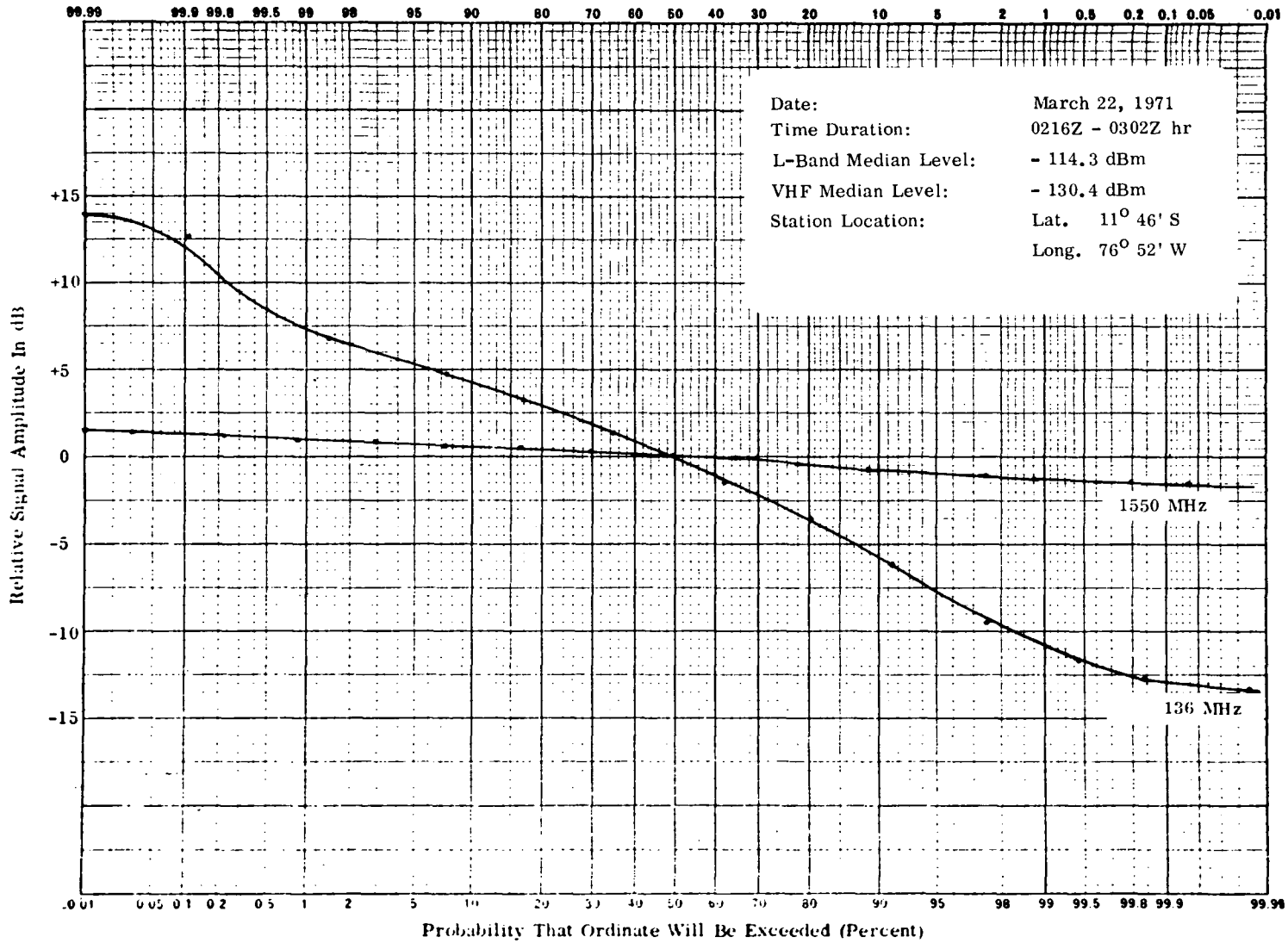

Figure B-23. Cumulative Amplitude Distribution of ATS-5 Signals

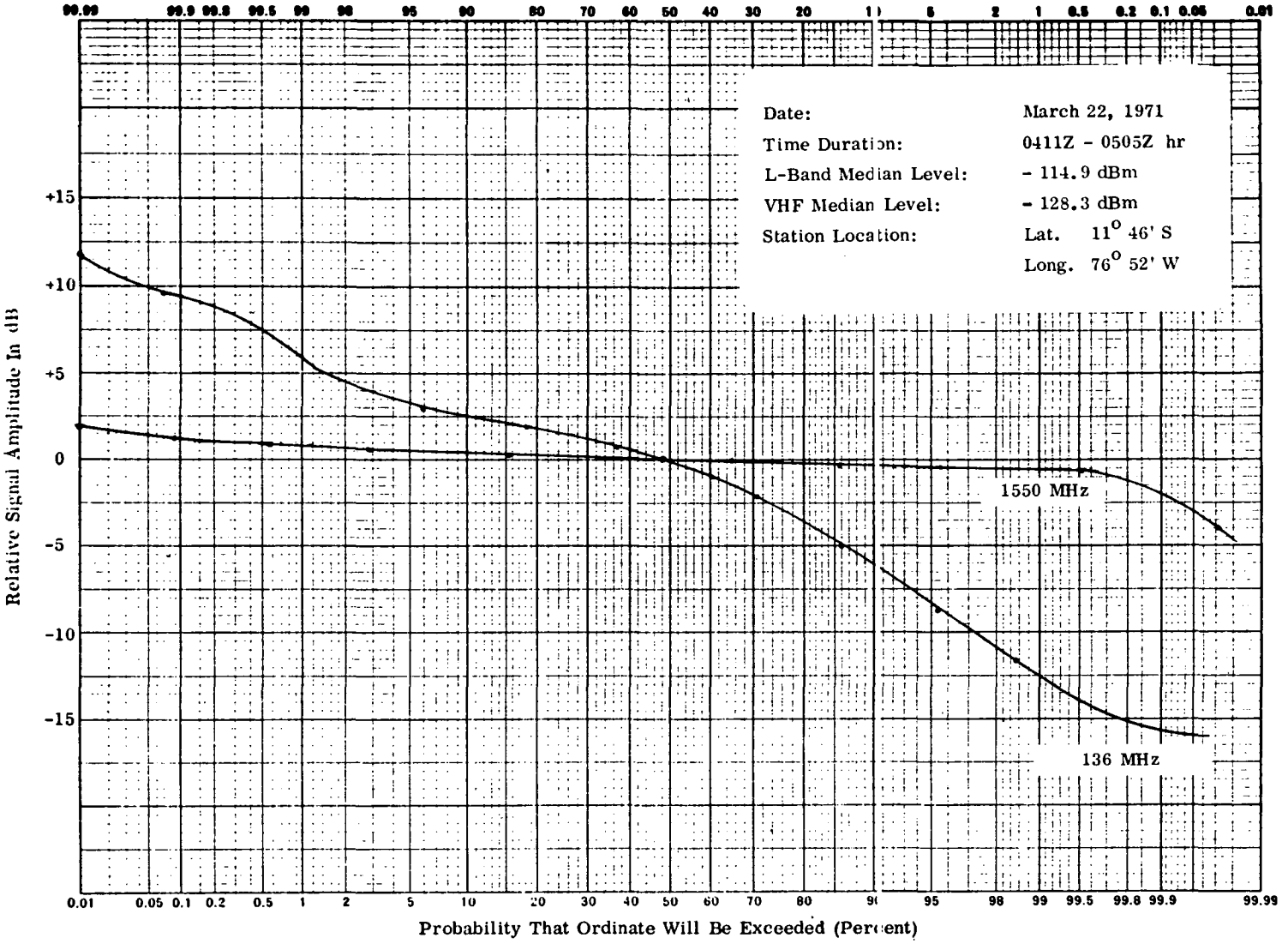

Figure B-24. Cumulative Amplitude Distribution of ATS-5 Signals

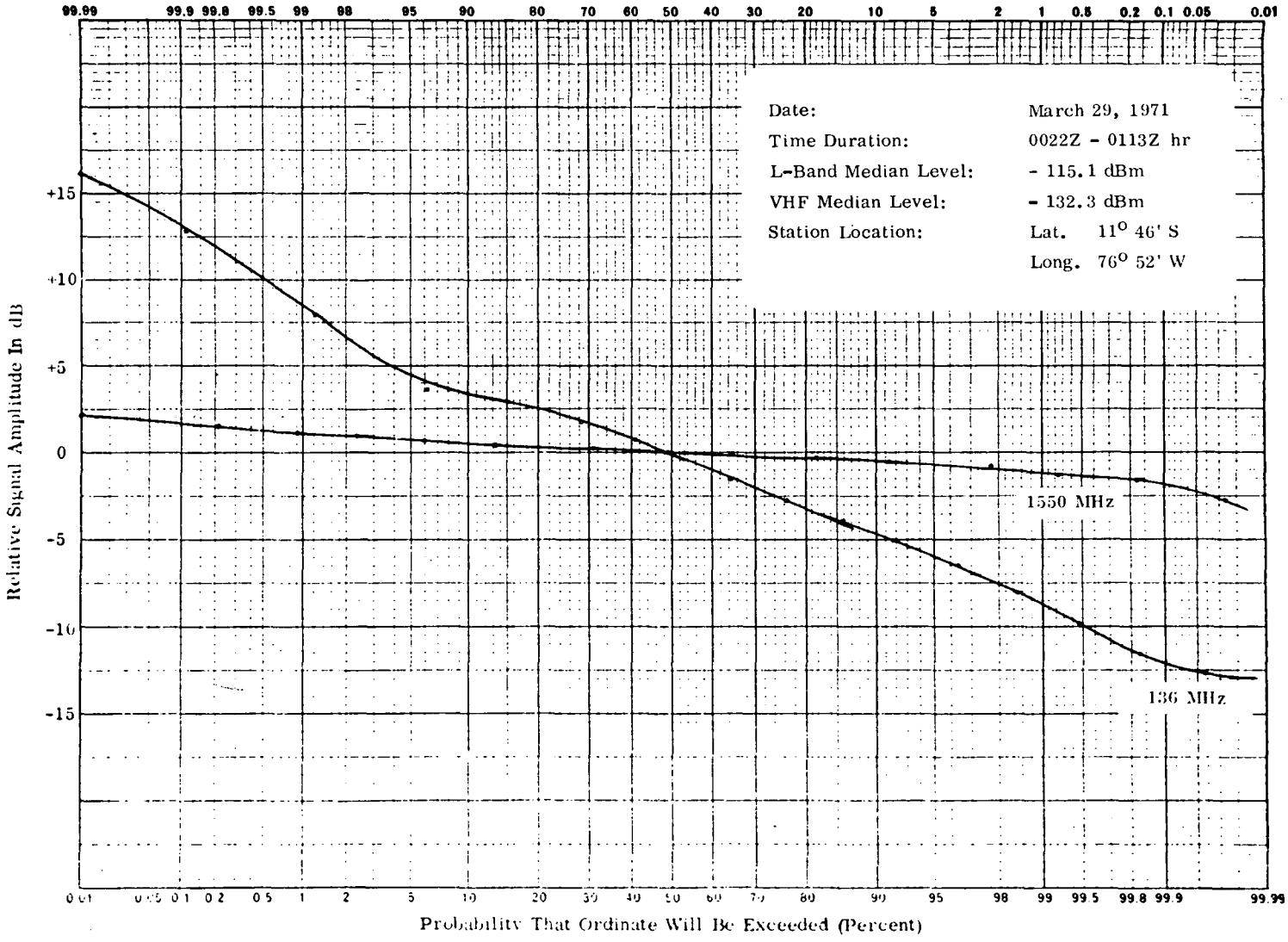

Figure B-25. Cumulative Amplitude Distribution of ATS-5 Signals

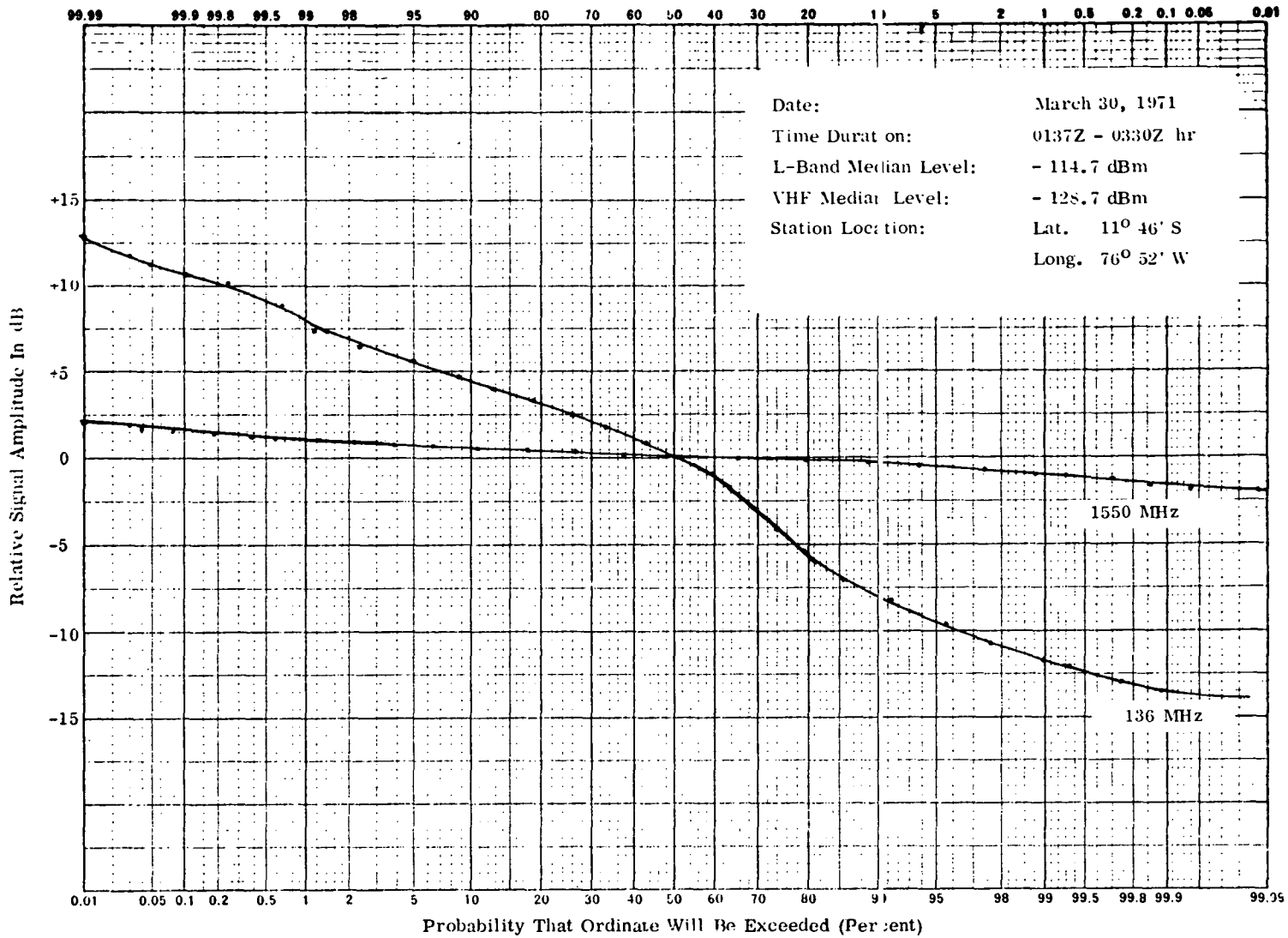

Figure B-26. Cumulative Amplitude Distribution of ATS-5 Signals

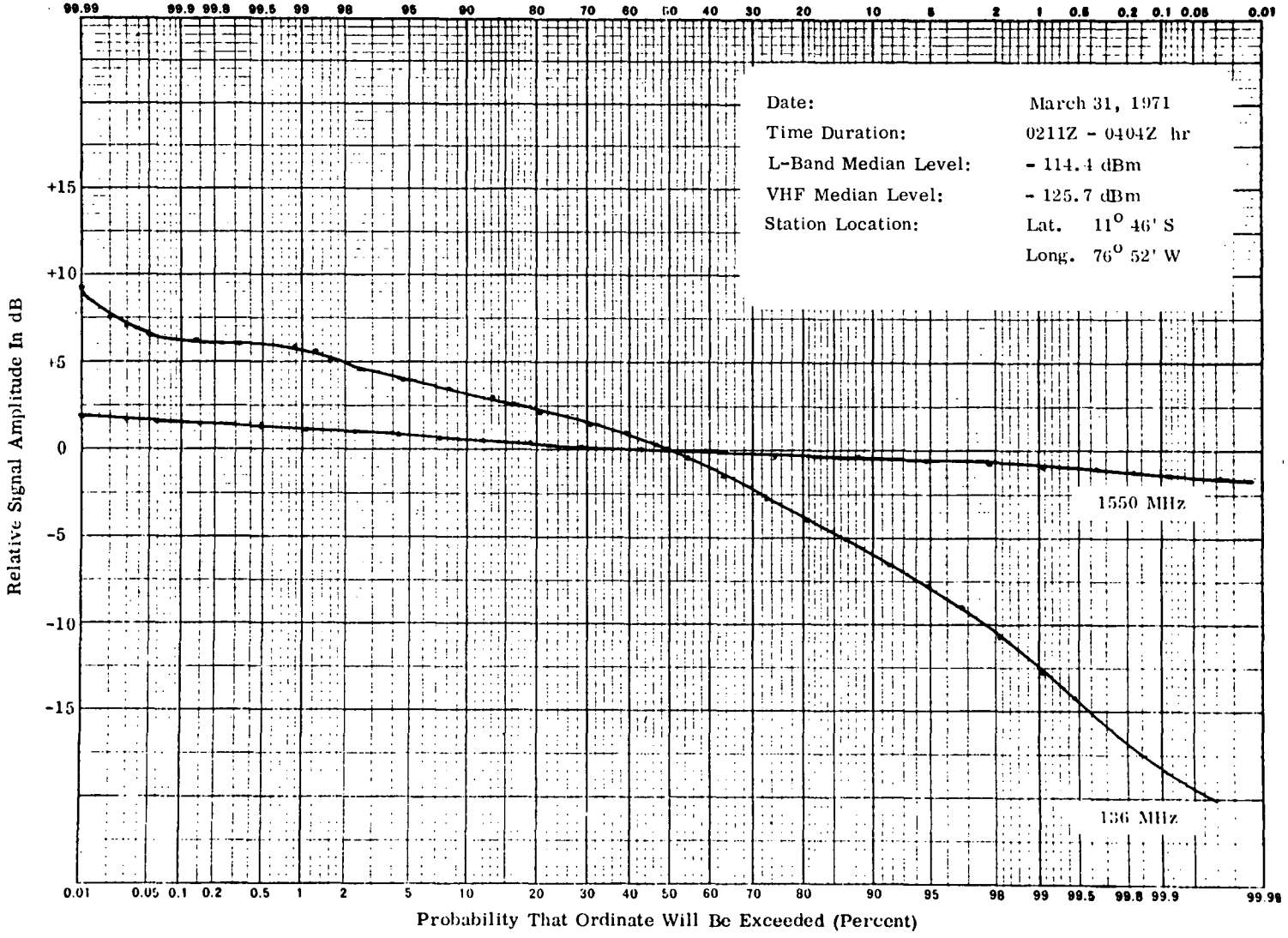

Figure B-27. Cumulative Amplitude Distribution of ATS-5 Signals

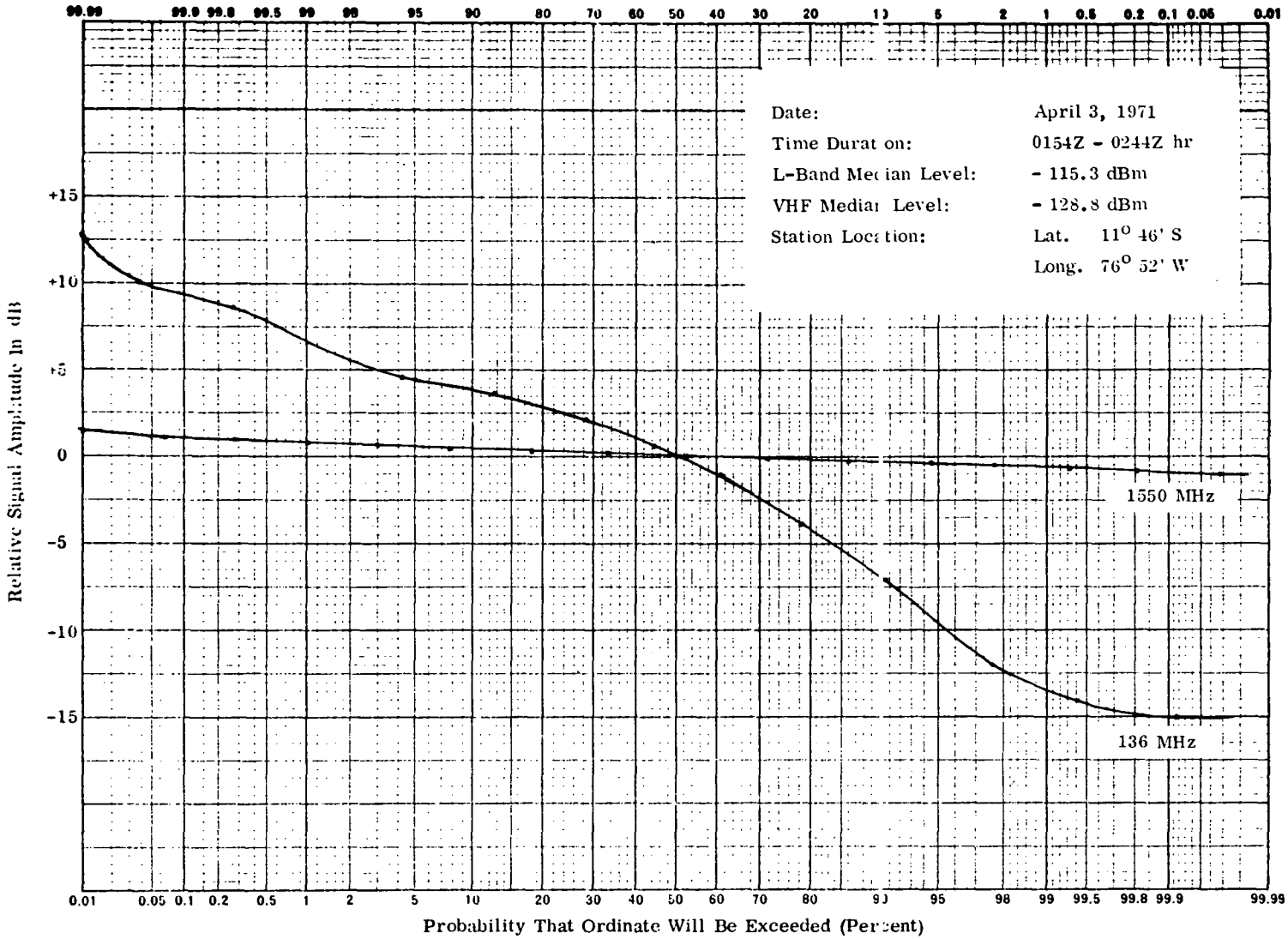

Figure B-28. Cumulative Amplitude Distribution of ATS-5 Signals

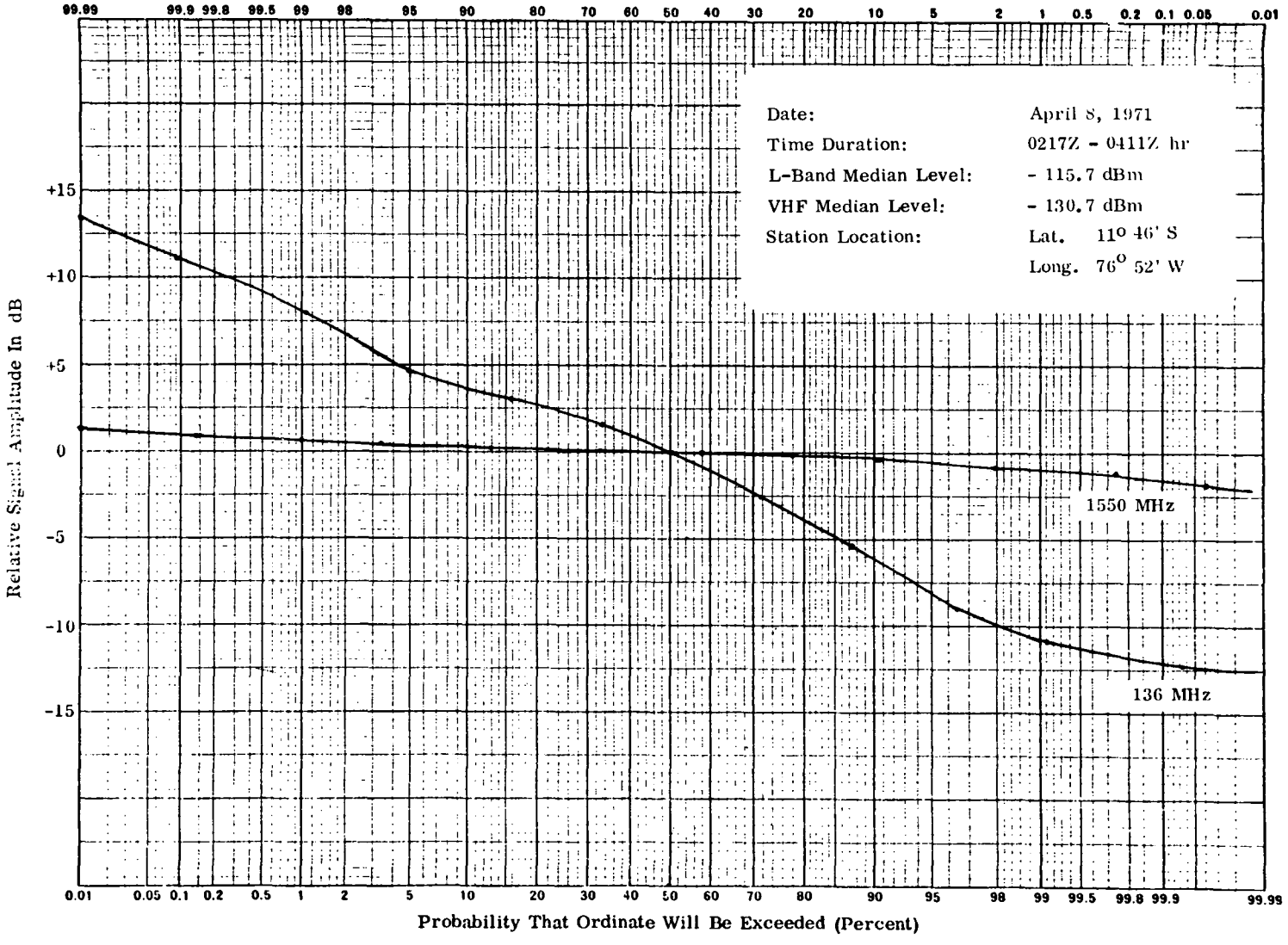

Figure B-29. Cumulative Amplitude Distribution of ATS-5 Signals

* U.S. GOVERNMENT PRINTING OFFICE: 1972-735-962/144